



Contents lists available at ScienceDirect

International Journal of Solids and Structures

journal homepage: www.elsevier.com/locate/ijsolstr

A comprehensive kinematic model of single-manifold Cosserat beam structures with application to a finite strain measurement model for strain gauges

Mayank Chadha, Michael D. Todd*

Department of Structural Engineering, University of California, San Diego 9500 Gilman Drive 0085 La, Jolla, CA 92093-0085 USA



ARTICLE INFO

Article history:

Received 11 January 2018

Revised 27 April 2018

Available online 20 September 2018

Keywords:

Coupled Poisson's and warping effect

Warping

Strain gauges

Cosserat beams

Finite strain

Large deformations

Shape sensing

Beam kinematics

ABSTRACT

In this paper, we investigate the coupling of Poisson's and warping effect for a general asymmetric cross-section of Cosserat beam. We present the challenges and inconsistencies observed as a result of our attempt to couple the two effects. The fully-coupled Poisson's transformation is then developed to describe the in-plane deformation for the prismatic beam. A comprehensive kinematic treatment of geometrically exact and nonlinear Cosserat beam subjected to large deformation and finite strain is finally obtained that extensively captures the deformation due to multiple curvatures, torsion, shear, axial deformation, warping and a fully-coupled Poisson's effect in the cross-section, all while maintaining the single manifold nature of the problem. The contributions to the strain vector and the deformation gradient tensor due to various deformation effects are interpreted and explained in detail. In the final part of the paper, we use the kinematics developed to establish a measurement model of discrete and finite length strain gauges attached to the surface of the beam (or embedded into the beam). We investigate the relationship between the scalar strain measurement of the strain gauge and the local finite strain parameters of the beam.

© 2018 Elsevier Ltd. All rights reserved.

1. Introduction

Strain measurement devices ("strain gages") are immensely important for a wide variety of measurement and monitoring applications ranging across civil structures, the energy sector, aerospace structures, and even biomedical systems, to name just a few. The development of sensing mechanisms that measure strain has been a well-developed field for over a century; the solutions have spanned piezo-resistive gages (arguably the most common and commercially-realized) to fiber optic systems to laser Doppler velocimetry (LDV). The sensing mechanism itself may require contact between the measuring device and structure (e.g., piezo-resistive gages or fiber optics) or be non-contact (e.g., LDV). Realizations of these architectures can result in localized measurements (discrete measurement points with a fixed length scale) or distributed measurements (e.g., fiber optic Rayleigh backscatter sensing [Friedman et al. \(2003\)](#), where the length scale and location of measurement depend on the optical pulsing).

A significant number of these monitoring applications for which strain measurements are required involve, fundamentally, one-dimensional slender structures, e.g., pipelines, suspension cables, tethers, surgical tubing, mooring cables, etc. The fundamental objective of this exposition is to develop a comprehensive kinematic model of such "single manifold" structures, based on Cosserat kinematics, and further develop a measurement model for the scalar strain of discrete and finite-length strain gauges assumed affixed to these kinds of structures. The measurement gauge length of the measuring device must be small enough to classify it as a discrete sensor. More specifically, we develop a geometrically exact non-linear kinematic model to capture warping (out of plane deformation), fully coupled Poisson's transformation (in-plane deformation) along with axial deformation of the midcurve, multiple curvatures, torsion and finite shear deformations in a Cosserat beam subjected to finite deformation and finite strain. This approach does not make the usual Euler-Bernoulli rigid cross-section assumption (plane cross-section remains plane after deformation). Instead, we propose a new approach to capture the coupled Poisson's and warping influence that is deformation-adaptive. We discuss the challenges associated with coupling Poisson's effect and warping. The proposed fully-coupled Poisson's effect captures the in-plane deformation of the cross-section. However, the

* Corresponding author.

E-mail addresses: machadha@eng.ucsd.edu (M. Chadha), mdtodd@ucsd.edu (M. D. Todd).

fully-coupled Poisson's transformation presented in this work does not model the in-plane deformation due to local buckling, which is a prominent phenomenon in case of thin-walled beam cross-sections. The work by Fang (2005) describes the in-plane cross-sectional distortion of thin-walled beam theory. Apart from this buckling limitation, the kinematics and the measurement model developed in this paper is completely general.

For a Cosserat beam subjected to the Euler-Bernoulli rigid cross-section assumption, the configuration of the beam is defined by the mid curve and the orthogonal body-centered director triad attached to the cross-section. The rigid cross-section assumption restricts the inclusion of Poisson's and warping effects. The problem of warping for various levels of complexities, from a simple Saint Venant problem (refer Sokolnikoff (1956)) to a complicated non-uniform asymmetric case (refer Trefftz (1935); Elter (1983); Burgoyne and Brown (1994); Brown and Burgoyne (1994); Simo and Vu-Quoc (1991); Vlasov (1961); Goodier (1941); Gjelsvik (1981); Lin and Hsiao (2003)), has been previously explored. We dedicate Section 2.3 to briefly review important contributions related to warping.

Per our survey of the literature, an investigation on the geometric coupling between the Poisson's effect and warping has not been attempted before. We believe that fully-coupled Poisson's and warping effect for a single-manifold beam problem will capture the in and out of the cross-sectional deformation with enhanced accuracy which is beneficial for both forward modeling analyses and solving inverse problems like shape sensing. The first step of this investigation aims at obtaining a simplified governing differential equation of warping from an assumed small displacement field. This step attempts to extend the theory of warping proposed by Brown and Burgoyne (1994) to incorporate the contribution of axial deformation and Poisson's effect to warping. We define a small displacement field including axial, bending, torsion and Poisson's effects for an asymmetric cross-section. We include the contribution due to bending because in a general asymmetric cross-section, the bending also contributes to warping. In general (refer to appendix A.1.5), the proposed warping function captures the non-linear bending-induced shear strain distribution across the cross-section, unlike Timoshenko's theory which assumes a constant shear distribution thereby preventing any out of plane deformation. The effect of warping due to non-linear shear induced by bending is quite significant in deep beams.

The governing differential equations for warping are obtained. However, the governing equation and the boundary condition at the periphery of the cross-section reflect an inconsistency if axial strain is included in the deformation field. We propose a solution to this inconsistency. Elimination of the observed inconsistency suggests a solution that does not include the effect of axial strain on warping explicitly, but we obtain a consistent modified differential equation for warping. We suggest two different solution approaches that have a separable variable form.

Obtaining the warping functions by solving various governing differential equations is beyond the scope of this current work, and the solution is assumed known in order to develop the fully-coupled Poisson's effect and establish the beam kinematics. Prior knowledge of the warping function guarantees the single manifold nature of the problem and allows us to obtain important parameters such as *deformation gradient tensor* and *Cauchy Green tensor* (or *Push-forward Riemann metric*) for the beam. Assuming that we know the solution to these differential equations, we propose a *fully-coupled Poisson's effect* that incorporates the effects of axial strain across the cross-section due to axial deformation, bending curvatures and warping. Henceforth, we call the effect attributed to the cross-sectional deformation (including in- and out-of-plane) a *fully-coupled Poisson's and warping effect*.

The strain vectors and the deformation gradient tensor of the deformed configuration referenced to both an initially straight beam configuration and an initially curved reference beam configuration are obtained. The contribution to each of these strain vectors due to different deformation effects are discussed in great detail. The kinematics of various restraint cases is obtained. In the view of authors, the kinematics developed herein establishes the most comprehensive geometry of Cosserat beam that still preserves the simplicity of the single-manifold nature of the problem.

We exploit the kinematics developed in the first half of the paper to develop a measurement model for the strain gauge attached on the surface of the beam or embedded in the beam. We arrive at the *Push-forward Riemannian Metric* of the beam that is key in developing the expression of the strain that would be detected by a finite length strain gauge. We validate our result by demonstrating the applicability of the expression obtained on a simple case of deformation that includes constant torsion, axial strain and Poisson's effect. We obtain the expression of scalar strain in the discrete strain gauge. We critically review the formula for the scalar strain proposed in our previous work on shape sensing based on the results obtained in this paper.

The mechanics of Cosserat structures is well developed and continues to be a topic of interest in the continuum mechanics community. We feel that the core reason of interest in this field lies in its mathematical simplicity. Cosserat rod theory developed by Cosserat and Cosserat (1909) is a powerful approach that attempts to capture the three-dimensional configuration of a slender rod by modeling the structure as a single manifold space curve (midcurve). Therefore, the local finite strain terms are the function of the arclength (manifold parameter) of the midcurve. The Cosserat description of the rods falls under the idea of Duhem (1893), where any point in the body is described by a position vector and by an attached set of vector triad called directors. An infinitesimal macro element of beam consists of many cross-sections. If Euler Bernoulli's rigid cross-section assumption is invoked, each section can be considered as a rigid body that can undergo translation and rotation. The translation is given by the mid-curve position vector and the rigid body rotation is obtained by the orthogonal rotation tensor (director triad). The smoothness in the rotation tensor and the midcurve position vector guarantees the continuity in the beam.

A detailed work on the extension of Cosserat continuum to develop a nonlinear theory of rods and shells was undertaken by Ericksen and Truesdell (1958). Kirchhoff is attributed to the idea of the finite displacement theory of rods, which was further improved by Hay (1942). Cohen (1966) developed a comprehensive non-linear static theory of elastic rods, which was extended by Whitman and DeSilva (1969) to include dynamics. The static finite strain beam theory for the plane case including shear deformation was developed by Reissner (1972, 1973, 1981). Simo (1985) extended the work of Reissner for a three-dimensional dynamic case using the director type of approach. Simo and Vu-Quoc (1991) developed the mechanics of Cosserat beam by incorporating the effect of warping for initially straight beams using the Saint Venant warping function (uniform torsion problem) including the effect of the unsymmetrical section by using the concept of shear center (refer Trefftz (1935) and Elter (1983)). They also obtained the finite deformation counterpart for the bi-shear and bi-moment in the linear thin-walled beam theory. Iura and Atluri (1989) obtained the governing equations for the initially curved beam configuration using virtual work principle. Kapania and Li (2003) presented a refined geometrically exact large deformation curved beam theory restricted to Euler Bernoulli's rigid cross-section. A more recent work by Meier et al. (2017) proposed a novel finite element formulation of geometrically-exact Kirchhoff-love theory and

presents a complete and detailed review of finite element analysis of geometrically-exact beams.

The two-part work by Green et al. (1974a,b) is one of the first expositions on the theory of elastic rods elucidated using classical three-dimensional equations and Cosserat curves. Readers may refer to the work of Naghdi and Rubin (1982), Brand and Rubin (2007) for the constraint theories of rods. The Cosserat rod is a special case of problems in micropolar continua, which is a special restraint case of micromorphic continua. The compiled work by Altenbach and Eremeyev (2013) serves as a great reference that cover topics on micro-polar continua (by Altenbach and Eremeyev), Cosserat rods (by Altenbach, Břisan and Eremeyev), micromorphic continua (by Samuel Forest), electromagnetism and generalized continua (by Maugin). The applications of Cosserat kinematics in modeling rod-like structure are multifaceted. For instance, Břisan and Altenbach (2011) describes an approach to model porous elastic rod, whereas Altenbach et al. (2012) presents the thermodynamic model of rods using Cosserat kinematics. Interested readers can refer to the detailed work and references by Antman (1972, 1995), Svetlitsky (2000, 2004), Maugin (2017) and Rubin (2000).

The earlier treatise we presented (Chadha and Todd (2017b)) serves as a detailed introduction to the variational formulation of Cosserat beam assuming Euler-Bernoulli's rigid cross-section assumption and reviews the development of the subject in great detail. Interested readers are recommended to refer to the references therein. Chadha and Todd (2017b) also defined the finite strain parameters that will be directly used in this paper. The kinematics described in this paper (and in many other papers like Simo (1985), Simo and Vu-Quoc (1991), Kapania and Li (2003) and Chadha and Todd (2017b)) incorporates finite shear, unlike the Kirchhoff-Love beam theory (refer to Antman (1974)) and can be thought of as a 3D large deformation generalization of Timoshenko's beam theory (refer to Timoshenko (1921)).

This work on the scalar surface strain can serve as a platform to help develop an optimization algorithm to investigate the orientation and placement of a strain gage array for single-manifold structures, and eventually reduce the approximation errors depending on the application. In the domain of continuum mechanics, the mechanics developed here offers a method to obtain finite strain parameters using the surface measurements. This is of utmost importance to develop a generalized (and more accurate) shape sensing methodology to obtain the global full-field deformed shape using limited set of finite surface strain measurement. The results presented here are in fact a part of developing a general shape sensing methodology that includes the effect of warping and Poisson's effect as an extension of authors previous work Todd et al. (2013) and Chadha and Chadha and Todd (2017a, 2018a, 2018b).

The remainder of the paper is arranged as follows: Section 2 details various deformed configurations, defines finite strain parameters, and explains the proposed coupled Poisson's and warping effects (a substantial portion on investigation on warping is discussed in Appendix A.1). Section 3 presents kinematics of the beam obtaining the general expression of the strain vector and deformation gradient tensor of the beam. Section 4 deals with measurement model for the strain gauges. The subsection 4.1 derives the expression of the scalar strain of finite length strain gauge and the subsection 4.2 deals with discrete strain gauge. In Section 5 we make concluding remarks.

2. Geometric description of various beam configurations

In wake of proposing the fully-coupled Poisson's and warping effect within our presentation of the kinematics, we define the following configurations of the beam:

1. Ω_0 : Curved reference beam configuration.
2. Ω_{00} : Mathematically straight beam configuration.
3. Ω_1 : Deformed configuration of the beam assuming Euler-Bernoulli's rigid cross-section.
4. Ω_2 : Deformed configuration of the beam allowing the cross-section to undergo out of plane warping only (no in-plane deformation).
5. Ω_3 : Deformed configuration of the beam including fully-coupled Poisson's and warping effect.

These configurations will be described in the subsequent sections. The nomenclature in this paper is slightly different from Chadha and Todd (2017b). Chadha and Todd (2017b) describes variational formulation of the configuration Ω_1 .

2.1. Description of the director frame and the midcurve

We brief the idea of the midcurve and director frame using the first three configurations along the lines of Chadha and Todd (2017b) for completion. We assume that the initial configuration (zero strain/zero stress state) is known and is the one in which the strain gauge is attached. We consider a fixed orthogonal triad $\{\mathbf{E}_i\}$. The deformed configuration Ω_1 assumes Euler-Bernoulli's rigid cross-section and is defined by the midcurve position vector $\boldsymbol{\varphi}(\xi_1)$ and the family of cross-sections $\blacksquare_1(\xi_1)$ with their boundaries $\Gamma_1(\xi_1)$, parametrized by the undeformed arc-length $\xi_1 \in [0, L_0]$. Here L_0 is the total length of the midcurve in the undeformed state Ω_0 or Ω_{00} . The midcurve is defined as the locus of the centroid of the family of cross-sections. The shape of the cross-section $\blacksquare_1(\xi_1)$ is independent of the deformation and its orientation is quantified by the set of orthogonal body centered Cosserat triad called directors $\{\mathbf{d}_i(\xi_1)\}$, such that

$$\boldsymbol{\varphi}(\xi_1) = \varphi_i \mathbf{E}_i; \quad \mathbf{d}_i(\xi_1) = d_{ij} \mathbf{E}_j. \quad (1)$$

Any point in the beam is defined by the material coordinates (ξ_1, ξ_2, ξ_3) that is independent of the beam configuration. The cross-section $\blacksquare_1(\xi_1) = \{(\xi_2, \xi_3) \in \mathbb{R}_{\xi_1}^2\}$, where $\mathbb{R}_{\xi_1}^2$ is 2D Euclidean space spanned by the directors $\mathbf{d}_2(\xi_1) - \mathbf{d}_3(\xi_1)$, with origin at the centroid of the cross-section $\blacksquare_1(\xi_1)$. A material point $(\xi_1, \xi_2, \xi_3) \in \Omega_1$ is defined by the position vector,

$$\mathbf{R}_1 = \boldsymbol{\varphi}(\xi_1) + \xi_2 \mathbf{d}_2(\xi_1) + \xi_3 \mathbf{d}_3(\xi_1). \quad (2)$$

The initially curved reference beam Ω_0 is defined by the director triad $\mathbf{d}_{0i}(\xi_1) = d_{0ij} \mathbf{E}_j$ and the midcurve position vector $\boldsymbol{\varphi}_0(\xi_1)$. Any point in Ω_0 is defined by the vector $\mathbf{R}_0 = \boldsymbol{\varphi}_0 + \xi_2 \mathbf{d}_{02} + \xi_3 \mathbf{d}_{03}$. It is convenient to mathematically define a straight beam configuration Ω_{00} such that the directors are defined by $\{\mathbf{E}_i\}$, the midcurve is a straight line along the vector \mathbf{E}_1 such that the midcurve position vector is defined by $\boldsymbol{\varphi}_{00} = \xi_1 \mathbf{E}_1$. Any point on the straight beam is then defined by $\mathbf{R}_{00} = \boldsymbol{\varphi}_{00} + \xi_2 \mathbf{E}_2 + \xi_3 \mathbf{E}_3 = \xi_i \mathbf{E}_i$. Note that the material point $(\xi_1, \xi_2, \xi_3) \in \Omega_{00}$ can be represented by writing $(\xi_2, \xi_3) \in \blacksquare_{00}(\xi_1)$. This notation will be used numerous times in the paper.

The triad $\{\mathbf{E}_i\}$, $\{\mathbf{d}_{0i}\}$ and $\{\mathbf{d}_i\}$ are related to each other by means of the orthogonal direction cosine tensor,

$$\mathbf{d}_i = \mathbf{Q} \mathbf{E}_i; \quad \mathbf{d}_{0i} = \mathbf{Q}_0 \mathbf{E}_i; \quad \mathbf{d}_i = \mathbf{Q}_r \mathbf{d}_{0i}, \quad (3)$$

such that the following relationships hold,

$$\mathbf{Q} = \mathbf{Q}_r \mathbf{Q}_0, \quad \mathbf{Q} = \mathbf{d}_i \otimes \mathbf{E}_i; \quad \mathbf{Q}_r = \mathbf{d}_i \otimes \mathbf{d}_{0i}; \quad \mathbf{Q}_0 = \mathbf{d}_{0i} \otimes \mathbf{E}_i. \quad (4)$$

Before we proceed further, we define the dot product between two vectors \mathbf{v}_1 and \mathbf{v}_2 as $\langle \mathbf{v}_1, \mathbf{v}_2 \rangle = v_{1i} v_{2i}$.

2.2. Description of the finite strain parameters defining the configuration Ω_1

The deformed configuration Ω_1 is subjected to axial deformation of the midcurve, shear deformations of the cross-section, torsion, and the bending curvatures. We define the deformed arc-length as s , the axial strain as $e(\xi_1)$, and the three shear angles as $\gamma_{11}(\xi_1)$, $\frac{\pi}{2} - \gamma_{12}(\xi_1)$ and $\frac{\pi}{2} - \gamma_{13}(\xi_1)$ subtended by the directors \mathbf{d}_1 , \mathbf{d}_2 and \mathbf{d}_3 with the tangent vector $\frac{\partial \varphi}{\partial s} = \boldsymbol{\varphi}_s$ respectively, as described in Chadha and Todd (2017b) such that

$$e = \frac{ds - d\xi_1}{d\xi_1} \Rightarrow \frac{d\xi_1}{ds} = \frac{1}{1+e};$$

$$\langle \boldsymbol{\varphi}_s, \mathbf{d}_i \rangle = \begin{cases} \cos \gamma_{1i}, & \text{for } i = 1 \\ \sin \gamma_{1i}, & \text{for } i = 2, 3 \end{cases} \quad (5)$$

Therefore,

$$\boldsymbol{\varphi}_{\xi_1} = (1 + e)(\cos \gamma_{11} \mathbf{d}_1 + \sin \gamma_{12} \mathbf{d}_2 + \sin \gamma_{13} \mathbf{d}_3). \quad (6)$$

Note that the above definitions do not uniquely define the shear angles. Interested readers may refer to Section 3.2 in Chadha and Todd (2017b), that describes a way to uniquely define the shear deformation. We define the axial strain vector $\boldsymbol{\epsilon}$ representing the strain due to shear and midcurve axial strain such that

$$\boldsymbol{\epsilon} = \boldsymbol{\varphi}_{\xi_1} - \mathbf{d}_1 = \bar{\epsilon}_i \mathbf{d}_i. \quad (7)$$

Mathematically, the curvatures in the beam are captured by the derivative of the director with respect to the arc-length. From Eq. 12 in Chadha and Todd (2017b), the following relations hold,

$$\mathbf{d}_{i,\xi_1} = \mathbf{Q}_{\xi_1} \mathbf{Q}^T \mathbf{d}_i = \mathbf{K} \mathbf{d}_i = \boldsymbol{\kappa} \times \mathbf{d}_i. \quad (8)$$

The tensor $\mathbf{Q}(\xi_1)$, represents the family of orthogonal tensors that belongs to the $SO(3)$ rotational Lie group. $\mathbf{Q}(\xi_1)$ can be understood as a curve in the manifold $SO(3)$, where $\mathbf{Q}_{\xi_1} \in T_{\mathbf{Q}}SO(3)$ represents the tangent vector to the curve $\mathbf{Q}(\xi_1)$ in $SO(3)$. Here, $T_{\mathbf{Q}}SO(3)$ represents the tangent space to $SO(3)$ at some $\mathbf{Q} \in SO(3)$. Note that $\mathbf{Q}_{\xi_1} \mathbf{Q}^T = \mathbf{K}(\xi_1)$ is the linear space of skew-symmetric matrix that has Darboux vector $\boldsymbol{\kappa}(\xi_1) = \bar{\kappa}_i \mathbf{d}_i$ as the corresponding axial vector, such that

$$\begin{bmatrix} \mathbf{d}_{1,\xi_1} \\ \mathbf{d}_{2,\xi_1} \\ \mathbf{d}_{3,\xi_1} \end{bmatrix} = \underbrace{\begin{bmatrix} 0 & \bar{\kappa}_3 & -\bar{\kappa}_2 \\ -\bar{\kappa}_3 & 0 & \bar{\kappa}_1 \\ \bar{\kappa}_2 & -\bar{\kappa}_1 & 0 \end{bmatrix}}_{\mathbf{K}^T} \begin{bmatrix} \mathbf{d}_1 \\ \mathbf{d}_2 \\ \mathbf{d}_3 \end{bmatrix}. \quad (9)$$

Here, $\bar{\kappa}_1$ represents the torsional curvature about the director \mathbf{d}_1 . The curvature terms $\bar{\kappa}_2$ and $\bar{\kappa}_3$ represent the curvature due to bending about the director \mathbf{d}_2 and \mathbf{d}_3 , respectively. For the configuration Ω_1 , $\boldsymbol{\varphi}(\xi_1) \in \mathbb{R}^3$ is sufficient to define the mid-curve, whereas the orientation of the cross-section is fully described by the director triad. Therefore, $\mathbb{R}^3 \times SO(3)$ is the configuration space for Ω_1 .

The geometric description of more general configurations $\Omega_2 - \Omega_3$ comprises of different families of cross-sections obtained by further transformation of the cross-section \blacksquare_1 . Therefore, before we continue to describe the configurations $\Omega_2 - \Omega_3$, we will first obtain the fully-coupled Poisson's and warping effect in the next three Sections 2.3–2.5.

2.3. An introductory remark on warping

The simplest non-trivial case of warping is Saint-Venant's uniformly torsion problem (refer p. 113 of Sokolnikoff (1956)) on a doubly symmetric prismatic bar subjected to a constant curvature $\bar{\kappa}_1(\xi_1) = \bar{\kappa}_1$. If the cross-section is not doubly symmetric, the torsion and bending are uncoupled by using the idea of shear-center. Elter (1983) describes two formulations of shear-center, the first

obtained using Saint-Venant's principle and the second attributed to Trefftz (1935). In Saint-Venant's principle, the distributed forces at the end-section (say $\blacksquare(L)$) are replaced by a statically equivalent concentrated force and couple. Trefftz (1935) proposed that the work done by the distributed forces at the end-section is equal to the work done by statically equivalent concentrated force and couple, thereby proposing equivalence in energy. Note that both the approaches are meant for uniform torsion.

Let the straight asymmetric beam be subjected to uniform torsion with constant curvature $\bar{\kappa}_1$. Let $\mathbf{n} = n_2 \mathbf{E}_2 + n_3 \mathbf{E}_3$ be the normal vector to the boundary $\Gamma(\xi_1)$ of the deformed cross-section $\blacksquare(\xi_1)$. Due to linear and small deformation nature of the problem, we express the displacement field in $\{\mathbf{E}_i\}$ frame. Let the position vector of the shear center from the centroid be $S_2 \mathbf{E}_2 + S_3 \mathbf{E}_3$. The corresponding linear displacement field \mathbf{u}_s measured about the shear center can be obtained as

$$\mathbf{u}_s = \bar{\kappa}_1 \xi_1 [\mathbf{E}_1 \times ((\xi_2 - S_2) \mathbf{E}_2 + (\xi_3 - S_3) \mathbf{E}_3)] + \bar{\kappa}_1 \Psi_s(\xi_2, \xi_3) \mathbf{E}_1. \quad (10)$$

The warping function may then be obtained by solving the following Neumann boundary value problem

$$\begin{aligned} \nabla^2 \Psi_s &= \Psi_{s,\xi_2 \xi_2} + \Psi_{s,\xi_3 \xi_3} = 0 \quad \text{on } \blacksquare(\xi_1); \\ \Psi_{s,n} &= \Psi_{s,\xi_2} n_2 + \Psi_{s,\xi_3} n_3 \\ &= -\langle ((\xi_2 - S_2) \mathbf{E}_2 + (\xi_3 - S_3) \mathbf{E}_3) \times \mathbf{n}, \mathbf{E}_1 \rangle \quad \text{on } \Gamma(\xi_1). \end{aligned} \quad (11)$$

The second last equation in Elter (1983) gives formula for the shear center, when the displacement field is expressed at any arbitrary point A other than the centroid. Considering the arbitrary point A to be the shear center S of the beam, we arrive at the following two conditions

$$\int_{\blacksquare} \xi_2 \Psi_s d\xi_2 d\xi_3 = \int_{\blacksquare} \xi_3 \Psi_s d\xi_2 d\xi_3 = 0. \quad (12)$$

Eqs. (11) and (12) can be solved to obtain S_2 , S_3 and Ψ_s , unique to a constant. Therefore, an additional normalization condition (that is also required for the axial force to vanish) can be invoked to solve for the constant,

$$\int_{\blacksquare} \Psi_s d\xi_2 d\xi_3 = 0. \quad (13)$$

Eqs. (11)–(13) gives a unique solution to the warping function Ψ_s for uniform torsion. Simo and Vu-Quoc (1991) use the warping function Ψ_s weighted by the warping amplitude $p(\xi_1)$ to consider non-uniform torsion in finite deformation problem. This adds an additional finite strain parameter $p(\xi_1)$, introducing the idea of bi-shear and bi-moment.

As indicated in Elter (1983), it is interesting to note that the warping function depends on the choice of origin. Consider the displacement field \mathbf{u} defined with respect to the centroid, which may be written as $\mathbf{u} = \bar{\kappa}_1 \xi_1 [\mathbf{E}_1 \times (\xi_2 \mathbf{E}_2 + \xi_3 \mathbf{E}_3)] + \bar{\kappa}_1 \Psi(\xi_2, \xi_3) \mathbf{E}_1$. The warping function $\Psi(\xi_2, \xi_3)$ is then obtained by solving the following differential equation

$$\begin{aligned} \nabla^2 \Psi &= 0 \quad \text{on } \blacksquare(\xi_1); \\ \Psi_{,n} &= -t \quad \text{on } \Gamma(\xi_1); \\ t &= \langle ((\xi_2 \mathbf{E}_2 + \xi_3 \mathbf{E}_3) \times \mathbf{n}), \mathbf{E}_1 \rangle. \end{aligned} \quad (14)$$

The location of the shear center can be obtained using a general Eq. (29) or Eq. (2) (for single and multi-connected regions), in Elter (1983).

Burgoyne and Brown (1994) presents a detailed theory of warping for non-uniform torsion considering symmetric cross-section. The assumed displacement field, where $W(\xi_1, \xi_2, \xi_3)$ represents the warping deformation, is written as

$$\begin{aligned} \mathbf{u} &= \theta(\xi_1) [\mathbf{E}_1 \times (\xi_2 \mathbf{E}_2 + \xi_3 \mathbf{E}_3)] + W(\xi_1, \xi_2, \xi_3) \mathbf{E}_1, \\ \theta(\xi_1) &= \theta(0) + \int_0^{\xi_1} \bar{\kappa}_1(\xi_1) d\xi_1. \end{aligned} \quad (15)$$

Here, θ represents the total twist angle. The governing differential equations for linear elasticity with Poisson's ratio $\nu = 0$ then become,

$$\begin{aligned} \nabla^2 W + \frac{E}{G} W_{,\xi_1 \xi_1} &= 0 \text{ on } \blacksquare(\xi_1); \\ W_{,n} &= -\theta_{,\xi_1} t \text{ on } \Gamma(\xi_1), \text{ such that,} \\ W_{,\xi_1} &= 0 \text{ or } \theta^{(r)} = 0 \text{ if the end is unrestrained in warping,} \\ &\text{where } r = 0, 2, 4, 6, \dots \\ W &= 0 \text{ or } \theta^{(r)} = 0 \text{ if the end is restrained in warping,} \\ &\text{where } r = 1, 3, 5, \dots \end{aligned} \tag{16}$$

Here, $\theta^{(r)}$ represents r order derivative of θ with respect to ξ_1 . For example, $\theta_{,\xi_1 \xi_1} = \theta^{(2)}$. Both these presentations of derivative are used interchangeably from here on. The parameters E and G are the Young's modulus and shear modulus, respectively. One of the two solution approaches proposed by Burgoyne and Brown (1994) is to use infinite series sum of the form

$$W(\xi_1, \xi_2, \xi_3) = \sum_{r=0}^{\infty} \theta^{(r)}(\xi_1) \Psi_r(\xi_2, \xi_3). \tag{17}$$

The idea is to solve for the functions Ψ_r , provided the twist angle $\theta(\xi_1)$ is known. This involves solving for Ψ_r that satisfies the following set of equations

$$\begin{aligned} \Psi_r &= 0 \text{ if } r \text{ is even or zero;} \\ \nabla^2 \Psi_1 &= 0 \text{ on } \blacksquare(\xi_1) \text{ and } \Psi_{1,n} = -t \text{ on } \Gamma(\xi_1); \\ \nabla^2 \Psi_r + \frac{E}{G} \Psi_{r-2} &= 0 \text{ on } \blacksquare(\xi_1) \text{ and } \Psi_{r,n} = 0 \text{ on } \Gamma(\xi_1) \\ &\text{for } r \geq 3. \end{aligned} \tag{18}$$

Knowing the functions $\Psi_r(\xi_2, \xi_3)$, we can estimate the warping deformation for large deformation beam problem as a finite sum

$$W(\xi_1, \xi_2, \xi_3) = \sum_{r=1}^n p^{(r-1)}(\xi_1) \Psi_r(\xi_2, \xi_3), \quad r \text{ is odd.} \tag{19}$$

The weighting parameter $p(\xi_1)$, is an additional unknown finite strain parameter known as the warping amplitude. To make sure that the higher derivatives of $p(\xi_1)$ are not additional unknowns, $p(\xi_1)$ is assumed to be at least C^{n-1} continuous.

A particularly notable work on the warping of a thin-walled open section for pure (non-uniform) torsion was presented by Vlasov (1961). Vlasov's theory considers the primary warping (or contour warping) but ignores the secondary warping (or thickness warping) of the cross-section. In Vlasov's theory, the line perpendicular to the contour remains perpendicular to the contour and undeformed in the deformed state (thus assuming Kirchhoff's thin plate assumption). Goodier (1941) and Gjelsvik (1981) incorporated the warping of walls of the beam with respect to the contour. The contour is defined as the intersection of the midsurface of wall with the cross-section (refer to Gjelsvik (1981)). Lin and Hsiao (2003) serves as an insightful reference to a complete derivation of torsional warping that includes both primary and secondary warping for a thin walled open section beam subjected to pure torsion. The warping function investigated in this paper is capable of capturing the out-of-plane deformation of thin-walled beams (refer Brown and Burgoyne (1994)).

The idea of shear center, center of twist, and their synonymic nature is debatable. The work by Brown and Burgoyne (1994) ignores the concept of shear-center and develops the coupled linear theory for torsion and flexure. They propose a trigonometric series solution for the governing equations to obtain the warping functions. As mentioned in Brown and Burgoyne (1994), the wide adaptation of the idea of the shear center by engineers can probably be attributed to its convenience. Their work critically reviews the idea of shear center and center of twist.

We now present our approach to model the coupling between the Poisson's effect and warping deformation. In Section 2.4 we attempt to extend the warping theory proposed by Burgoyne and Brown (1994) and Brown and Burgoyne (1994) to incorporate the effect of axial strain and Poisson's deformation into the warping. Therefore, Section 2.4 along with the appendix A.1 elucidates the first stage of this coupling. In Section 2.5, we further refine the coupling by defining the fully-coupled Poisson's transformation.

2.4. Coupling between axial strain, Poisson's effect and warping

As discussed before, the warping function is obtained for the linear elastic case and suitably modified to capture non-linear cases. Motivated from the work of Brown and Burgoyne (1994), we assume a linear small deformation field including non-uniform torsion, bending, axial deformation and Poisson's effect for asymmetric problem. For a general asymmetric cross-section, bending induces warping, causing a coupling between bending and torsion. The incorporation of axial deformation helps us to investigate the influence of Poisson's effect and axial strain on warping (but not vice-versa, that is taken care of by the second stage of coupling, as we shall see later). We consider an asymmetric cross-section subjected to bending, axial deformation of midcurve, torsion, and warping in the sense of small deformation. Hence, consider a displacement field

$$\begin{aligned} u_1 &= W(\xi_1, \xi_2, \xi_3) - \xi_2 \left(\int \bar{\kappa}_3(\xi_1) d\xi_1 + C_1 \right) \\ &\quad + \xi_3 \left(\int \bar{\kappa}_2(\xi_1) d\xi_1 + C_2 \right) + \left(\int e(\xi_1) d\xi_1 + C_3 \right); \\ u_2 &= \left[\int \int \bar{\kappa}_3(\xi_1) d\xi_1 d\xi_1 + C_1 \xi_1 + C_4 \right] \\ &\quad - \xi_3 \left(\int \bar{\kappa}_1(\xi_1) d\xi_1 + C_5 \right) - \nu e(\xi_1) \xi_2; \\ u_3 &= - \left[\int \int \bar{\kappa}_2(\xi_1) d\xi_1 d\xi_1 + C_2 \xi_1 + C_6 \right] \\ &\quad + \xi_2 \left(\int \bar{\kappa}_1(\xi_1) d\xi_1 + C_5 \right) - \nu e(\xi_1) \xi_3. \end{aligned} \tag{20}$$

Here, $C_1 - C_6$ are the constants that depend on the boundary conditions and the initial undeformed state of the beam. The non-zero components of isotropic elastic stress tensor including the Poisson's effect can be obtained from Eq. (20) as

$$\begin{aligned} \sigma_{11} &= \tilde{\lambda}(W_{,\xi_1} + \xi_3 \bar{\kappa}_2 - \xi_2 \bar{\kappa}_3) + (\tilde{\lambda} - 2\lambda\nu)e; \\ \sigma_{12} &= \sigma_{21} = G(W_{,\xi_2} - \xi_3 \bar{\kappa}_1 - \nu \xi_2 e_{,\xi_1}); \\ \sigma_{13} &= \sigma_{31} = G(W_{,\xi_3} + \xi_2 \bar{\kappa}_1 - \nu \xi_3 e_{,\xi_1}); \\ \sigma_{22} &= \lambda(W_{,\xi_1} + \xi_3 \bar{\kappa}_2 - \xi_2 \bar{\kappa}_3) - (\nu \tilde{\lambda} + \lambda(\nu - 1))e; \\ \sigma_{33} &= \lambda(W_{,\xi_1} + \xi_3 \bar{\kappa}_2 - \xi_2 \bar{\kappa}_3) - (\nu \tilde{\lambda} + \lambda(\nu - 1))e. \end{aligned} \tag{21}$$

Here, $\lambda = \frac{\nu E}{(1+\nu)(1-2\nu)}$ and $\tilde{\lambda} = 2G + \lambda$. The parameters E , G and ν are Young's modulus, shear modulus and Poisson's ratio respectively. Note that $\lim_{\nu \rightarrow 0} \sigma_{22} = 0$ and $\lim_{\nu \rightarrow 0} \sigma_{33} = 0$. We restrict ourselves to stress-equilibrium in the E_1 direction, as we are interested in solving for the warping function. Therefore, the governing differential equations are

$$\begin{aligned} \sigma_{1,j,j} &= 0 \Rightarrow \nabla^2 W \\ &\quad + \frac{\tilde{\lambda}}{G} (W_{,\xi_1 \xi_1} - \xi_2 \bar{\kappa}_{3,\xi_1} + \xi_3 \bar{\kappa}_{2,\xi_1}) + \bar{\lambda} e_{,\xi_1} = 0 \text{ on } \blacksquare(\xi_1); \end{aligned} \tag{22a}$$

$$W_{,\mathbf{n}} = \bar{\kappa}_1 \overbrace{\left[\mathbf{n} \times (\xi_2 \mathbf{E}_2 + \xi_3 \mathbf{E}_3) \right]}^{-t} \cdot \mathbf{E}_1 + e_{,\xi_1} \nu \overbrace{\left[\mathbf{n} \cdot (\xi_2 \mathbf{E}_2 + \xi_3 \mathbf{E}_3) \right]}^t \quad \text{on } \Gamma(\xi_1). \quad (22b)$$

Here, $\bar{\lambda} = \frac{\tilde{\lambda} + 2\nu(G - \tilde{\lambda})}{G}$. As Eq. (1) in Brown and Burgoyne (1994), we define the stress resultants for axial force, bending moment and torsion at the centroid as follows

$$\begin{aligned} P_1(\xi_1) &= \int_{\blacksquare(\xi_1)} \sigma_{11} d\xi_2 d\xi_3 = (\tilde{\lambda} - 2\lambda\nu)Ae + \tilde{\lambda} \int_{\blacksquare(\xi_1)} W_{,\xi_1} d\xi_2 d\xi_3 \\ T(\xi_1) &= \int_{\blacksquare(\xi_1)} (\xi_2 \sigma_{13} - \xi_3 \sigma_{12}) d\xi_2 d\xi_3 = GJ\bar{\kappa}_1 \\ &\quad + G \int_{\blacksquare(\xi_1)} (\xi_2 W_{,\xi_3} - \xi_3 W_{,\xi_2}) d\xi_2 d\xi_3; \\ M_2(\xi_1) &= \int_{\blacksquare(\xi_1)} \xi_3 \sigma_{11} d\xi_2 d\xi_3 \\ &= \tilde{\lambda} \left(\int_{\blacksquare(\xi_1)} \xi_3 W_{,\xi_1} d\xi_2 d\xi_3 + I_{22}\bar{\kappa}_2 - I_{23}\bar{\kappa}_3 \right); \\ M_3(\xi_1) &= \int_{\blacksquare(\xi_1)} \xi_2 \sigma_{11} d\xi_2 d\xi_3 \\ &= \tilde{\lambda} \left(- \int_{\blacksquare(\xi_1)} \xi_2 W_{,\xi_1} d\xi_2 d\xi_3 + I_{33}\bar{\kappa}_3 - I_{23}\bar{\kappa}_2 \right), \end{aligned} \quad (23)$$

where $A(\xi_1) = \int_{\blacksquare} d\xi_2 d\xi_3$, $I_{ij} = \int_{\blacksquare} \xi_i \xi_j d\xi_2 d\xi_3$ for $i = 2, 3$ and $J = I_{22} + I_{33}$.

The warping differential Eq. (22a) across the cross-section $\blacksquare(\xi_1)$ is inconsistent with the peripheral boundary condition (22b). To avoid a sharp deviation from the prime topic of the paper (“comprehensive kinematics of Cosserat beam”), we discuss this inconsistency, solution procedure, and challenges associated with solving for the function $W(\xi_1, \xi_2, \xi_3)$ in Appendix A.1 for the interested reader.

To proceed further, we assume that the warping function $W(\xi_1, \xi_2, \xi_3)$ can be expressed in a variable separable form (for instance, of form $p(\xi_1)\Psi(\xi_2, \xi_3)$) and the cross-sectional dependence of warping function (the function $\Psi(\xi_2, \xi_3)$) is known. Prior knowledge of $\Psi(\xi_2, \xi_3)$ guarantees the single manifold nature of the kinematics. In appendix A.1.6, we propose a simplified form of the warping function $W(\xi_1, \xi_2, \xi_3)$ that can be used to capture bending-induced shear warping and torsion warping in the beams subjected to large deformations. To understand the second stage of coupling, we need to define the deformed cross-sections Ω_2 and Ω_3 .

2.5. Description of the configuration Ω_2 and Ω_3

The configuration Ω_2 is defined by the midcurve $\varphi(\xi_1)$ and non-planar family of warped cross-sections (as discussed in Section 2.4) $\blacksquare_2(\xi_1) \subset \mathbb{R}_{\xi_1}^3$, where $\mathbb{R}_{\xi_1}^3$ is a three-dimensional Euclidean space spanned by the director triad $\{\mathbf{d}_i(\xi_1)\}$ with its origin at the centroid of the cross-section $\blacksquare_1(\xi_1)$ (refer Fig. 1). Therefore, if $(W(\xi_1, \xi_2, \xi_3), \xi_2, \xi_3) \in \blacksquare_2(\xi_1)$, we can define a differentiable map $M_{12\xi_1} : \blacksquare_1(\xi_1) \rightarrow \blacksquare_2(\xi_1)$ such that

$$M_{12\xi_1} : (\xi_2, \xi_3) \mapsto (W(\xi_1, \xi_2, \xi_3), \xi_2, \xi_3). \quad (24)$$

Note that the projection of the cross-section $\blacksquare_2(\xi_1)$ onto the $\mathbb{R}_{\xi_1}^2$ space yields $\blacksquare_1(\xi_1)$, implying no in plane deformation. The position vector for any point in Ω_2 is,

$$\mathbf{R}_2(\xi_1, \xi_2, \xi_3) = \varphi(\xi_1) + \xi_2 \mathbf{d}_2(\xi_1) + \xi_3 \mathbf{d}_3(\xi_1) + W(\xi_1, \xi_2, \xi_3) \mathbf{d}_1(\xi_1).$$

(25)

We now describe the most general configuration that includes fully-coupled Poisson’s and warping effect. The configuration Ω_3 is defined by the midcurve $\varphi(\xi_1)$ and the family of non-planar cross-sections $\blacksquare_3(\xi_1) \subset \mathbb{R}_{\xi_1}^3$ such that $\blacksquare_3(\xi_1) = \{(W(\xi_1, \xi_2, \xi_3), \xi_2, \xi_3) \in \mathbb{R}_{\xi_1}^3\}$. We define the planar cross-section $\blacksquare_4(\xi_1) = \{(\hat{\xi}_2, \hat{\xi}_3) \in \mathbb{R}_{\xi_1}^2\}$ subjected to only in-plane Poisson’s deformation. For a point $(\xi_2, \xi_3) \in \blacksquare_1(\xi_1)$ and $(\hat{\xi}_2, \hat{\xi}_3) \in \blacksquare_4(\xi_1)$, we define Poisson’s transformation $P_{\xi_1} : \blacksquare_1(\xi_1) \rightarrow \blacksquare_4(\xi_1)$ such that

$$\begin{aligned} P_{\xi_1} : (\xi_2, \xi_3) &\mapsto (\hat{\xi}_2, \hat{\xi}_3) \\ \hat{\xi}_i &= \left(1 - \nu(\xi_1, \xi_2, \xi_3)(\lambda_1^2, \mathbf{d}_i)\right) \xi_i \quad \text{for } i = 2, 3. \end{aligned} \quad (26)$$

Here, $\nu(\xi_1, \xi_2, \xi_3)$ is the Poisson’s ratio for the assumed isotropic material. However, we will assume that the material is homogeneous for further discussion, thus taking a constant Poisson’s ratio $\nu(\xi_1, \xi_2, \xi_3) = \nu$. The quantity λ_1^2 represents the first strain vector of the deformed configuration Ω_2 and will be discussed in Section 3.1. The position vector for any material point in Ω_3 is

$$\mathbf{R}_3 = \varphi(\xi_1) + \hat{\xi}_2 \mathbf{d}_2(\xi_1) + \hat{\xi}_3 \mathbf{d}_3(\xi_1) + W(\xi_1, \xi_2, \xi_3) \mathbf{d}_1(\xi_1). \quad (27)$$

This completes our endeavor to obtain fully-coupled Poisson’s and warping effect. Fig. 1 describes various deformed configurations of the beam. To develop the kinematics of the beam and investigate the mechanics of strain gauges, we need to define certain geometric structures associated with the beam.

2.6. Surface bounding the beam and the associated tangent space

From here on, we use the index j to represent any entity related to the deformed configuration Ω_j with $j = 1 - 3$. No sum is implied on j throughout the paper.

Section 4 discusses the geometry of the beam surface where the surface strain gauge is attached. Therefore, we define \mathfrak{S}_{00} , \mathfrak{S}_0 and \mathfrak{S}_j as the surface bounding the beam Ω_{00} , Ω_0 and Ω_j respectively (not including the bounding cross-sections at the two ends of the beam). Assuming that the patch of these surfaces on which strain gauge is attached is smooth and continuous, we can consider \mathfrak{S}_{00} , \mathfrak{S}_0 and \mathfrak{S}_j as regular surfaces which are manifold of dimension 2. The configurations Ω_{00} , Ω_0 and Ω_j are manifolds of dimension 3 (essentially Euclidean space \mathbb{R}^3).

We define the deformation map $\phi_j : \Omega_{00} \rightarrow \Omega_j$. Since \mathfrak{S}_{00} represents the boundary of the undeformed state Ω_{00} , we can define the map $\phi_j|_{\mathfrak{S}_{00}} = \tilde{\phi}_j$ (mapping ϕ_j restricted to the manifold \mathfrak{S}_{00}), such that $\tilde{\phi}_j : \mathfrak{S}_{00} \rightarrow \mathfrak{S}_j$. We represent a tangent space of the manifold M at point $a \in M$ as $T_a M$. The differential map $d\phi_j : T_p \Omega_{00} \rightarrow T_{\phi_j(p)} \Omega_j$ and $d\tilde{\phi}_j : T_q \mathfrak{S}_{00} \rightarrow T_{\tilde{\phi}_j(q)} \mathfrak{S}_j$ is homeomorphism and has rank 3 and 2 respectively, for all $p \in \Omega_{00}$ and $q \in \mathfrak{S}_{00}$ (assuming no cracks or dislocations and a continuous beam). Despite the fact that $\phi_j \equiv \mathbf{R}_j$, we did not define the deformation map as \mathbf{R}_j because that would imply the differential map to be $d\mathbf{R}_j$. However, we will use $d\mathbf{R}_j$ to define an infinitesimal tangent vector for the definition of deformation gradient tensor (as is customary in continuum mechanics). Fig. 2 illustrates the idea discussed in this section.

3. Kinematics: Deformation gradient tensor and strain vector

In this section, we arrive at the deformation gradient tensor \mathbf{F}_j and three strain vectors λ_i^j (with $i = 1 - 3$) of the beam configuration Ω_j referenced to the straight beam configuration Ω_{00} . In Section 3.4, we derive the deformation gradient tensor \mathbf{F}_j^r and the strain vectors $\lambda_i^{r,j}$ of the beam configuration Ω_j referenced to the initially curved reference configuration Ω_0 .

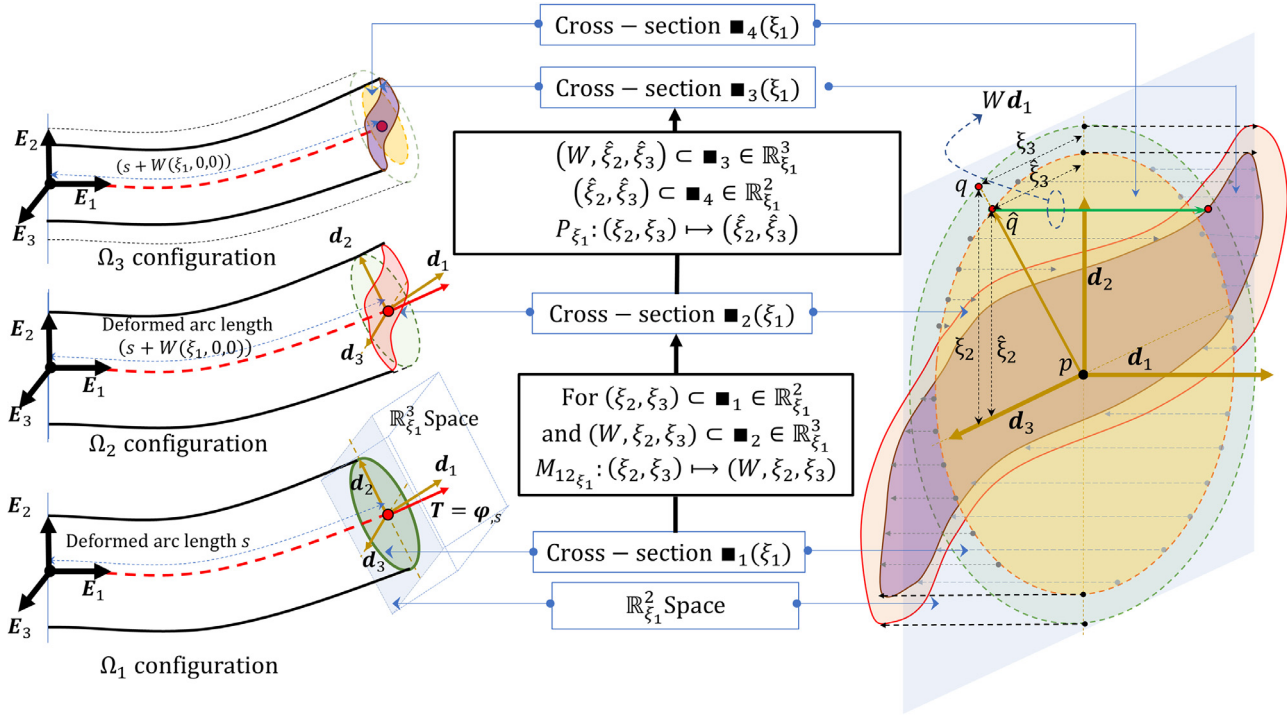


Fig. 1. Schematic diagram showing geometric description of configurations Ω_1 , Ω_2 and Ω_3 .

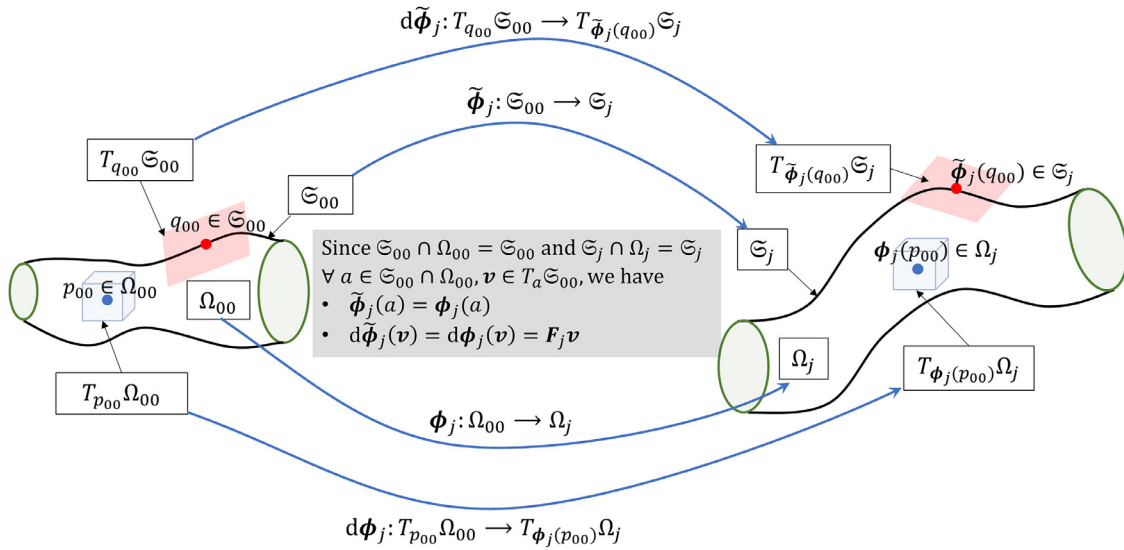


Fig. 2. Mathematical structures and various mappings associated with the beam configurations.

3.1. Deformation gradient tensor and the strain vectors

Consider infinitesimal vector $d\mathbf{R}_{00} = d\xi_i \mathbf{E}_i \in T_p \Omega_{00}$ (or in $T_p \mathfrak{S}_{00}$) that deforms to $d\mathbf{R}_j \in T_{\phi_j(p)} \Omega_j$ (or in $T_{\tilde{\phi}_j(p)} \mathfrak{S}_j$). If $p \in \Omega_{00}$ we have differential map $d\phi_j: d\mathbf{R}_{00} \mapsto d\mathbf{R}_j$, else if $p \in \mathfrak{S}_{00}$, then $d\tilde{\phi}_j: d\mathbf{R}_{00} \mapsto d\mathbf{R}_j$.

The deformation gradient tensor F_j maps a tangent vector from undeformed configuration to the deformed configuration. Since $\mathfrak{S}_{00} \cap \Omega_{00} = \mathfrak{S}_{00}$ (and $\mathfrak{S}_j \cap \Omega_j = \mathfrak{S}_j$), for any $p \in \mathfrak{S}_j \cap \Omega_j$, we have $\phi_j(p) = \tilde{\phi}_j(p)$. The tangent space on surface has the dimension 2, whereas the tangent space on the deformed (or undeformed) configuration has the dimension 3. But we can express any vector (which is a geometric object) in either $\{\mathbf{E}_i\}$ or $\{\mathbf{d}_i\}$ frame. Hence, for any vector $v \in (T_p \Omega_{00} \cap T_p \mathfrak{S}_{00})$, at the point $p \in (\Omega_{00} \cap \mathfrak{S}_{00})$, we

have $d\phi_j(v) = d\tilde{\phi}_j(v) = F_j v$. Thus the expression of scalar strain developed for a surface-mounted strain gauge in Section 4 is applicable to the strain gauge embedded in the beam as well.

From Eq. (23) of Chadha and Todd (2017b),

$$F_j = \frac{d\mathbf{R}_j}{d\mathbf{R}_{00}} = \mathbf{R}_{j,\xi_i} \otimes \mathbf{E}_i. \quad (28)$$

For $j = 1$, the first component of infinitesimal vector $d\mathbf{R}_{00}$ strains, whereas the other two components just experience rotation because of Euler–Bernoulli's rigid cross-section assumption in the configuration Ω_1 (refer section 3.1.1 of Chadha and Todd (2017b)). For $j \neq 1$, the second and the third component of the infinitesimal vector $d\mathbf{R}_{00}$ strains as well, owing to the coupled Poisson's and

warping effect. Thus we define,

$$\frac{\partial \mathbf{R}_j}{\partial \xi_i} = \boldsymbol{\lambda}_i^j + \mathbf{d}_i. \tag{29}$$

Here, $\boldsymbol{\lambda}_i^j$ represents i^{th} strain vector in the Ω_j configuration. Therefore, from Eqs. (4), (28) and (29), we can write the expression of deformation gradient tensor for the configuration Ω_j referenced to the configuration Ω_{00} as

$$\mathbf{F}_j = (\boldsymbol{\lambda}_i^j + \mathbf{d}_i) \otimes \mathbf{E}_i = \boldsymbol{\lambda}_i^j \otimes \mathbf{E}_i + \mathbf{Q}. \tag{30}$$

The deformation gradient tensor \mathbf{F}_j can be written as

$$\begin{aligned} \mathbf{F}_j &= \mathbf{V}_j \mathbf{Q} = \mathbf{Q} \mathbf{U}_j; \\ \mathbf{V}_j &= \boldsymbol{\lambda}_i^j \otimes \mathbf{d}_i + \mathbf{I}_3; \\ \mathbf{U}_j &= \bar{\boldsymbol{\lambda}}_i^j \otimes \mathbf{E}_i + \mathbf{I}_3. \end{aligned} \tag{31}$$

Here, $\bar{\boldsymbol{\lambda}}_i^j = \mathbf{Q}^T \boldsymbol{\lambda}_i^j$ is the material form of the vector $\boldsymbol{\lambda}_i^j$ (refer section 2.2.3 of Chadha and Todd (2017b)). The vector \mathbf{V}_j and \mathbf{U}_j represent the left stretch tensor and right stretch tensor, respectively, for the deformed state Ω_j referenced to the configuration Ω_{00} . In component form, the deformation gradient tensor and the stretch tensors can be written as

$$\begin{aligned} [\mathbf{F}_j]_{\mathbf{d}_p \otimes \mathbf{E}_q} &= [\bar{\mathbf{F}}_j]_{\mathbf{E}_p \otimes \mathbf{E}_q} = [\mathbf{U}_j]_{\mathbf{E}_p \otimes \mathbf{E}_q} = [\mathbf{V}_j]_{\mathbf{d}_p \otimes \mathbf{E}_q} \\ &\text{displacement gradient tensor } [\nabla_{\Omega_{00}} \mathbf{u}_j]_{\mathbf{d}_p \otimes \mathbf{E}_q} \\ &= \overbrace{\begin{bmatrix} \langle \boldsymbol{\lambda}_1^j, \mathbf{d}_1 \rangle & \langle \boldsymbol{\lambda}_2^j, \mathbf{d}_1 \rangle & \langle \boldsymbol{\lambda}_3^j, \mathbf{d}_1 \rangle \\ \langle \boldsymbol{\lambda}_1^j, \mathbf{d}_2 \rangle & \langle \boldsymbol{\lambda}_2^j, \mathbf{d}_2 \rangle & \langle \boldsymbol{\lambda}_3^j, \mathbf{d}_2 \rangle \\ \langle \boldsymbol{\lambda}_1^j, \mathbf{d}_3 \rangle & \langle \boldsymbol{\lambda}_2^j, \mathbf{d}_3 \rangle & \langle \boldsymbol{\lambda}_3^j, \mathbf{d}_3 \rangle \end{bmatrix}} + \begin{bmatrix} 1 & 0 & 0 \\ 0 & 1 & 0 \\ 0 & 0 & 1 \end{bmatrix}; \\ [\mathbf{F}_j]_{\mathbf{d}_p \otimes \mathbf{E}_q} &= \langle \boldsymbol{\lambda}_i^j, \mathbf{d}_p \rangle + \delta_{pq}. \end{aligned} \tag{32}$$

The notation $[\mathbf{F}_j]_{\mathbf{d}_p \otimes \mathbf{E}_q}$ implies that in the operation $\mathbf{F}_j \cdot \mathbf{d}\mathbf{R}_{00} = \mathbf{d}\mathbf{R}_j$, the component of the vector $\mathbf{d}\mathbf{R}_{00}$ is expressed in $\{\mathbf{E}_i\}$ frame and the components of the vector $\mathbf{d}\mathbf{R}_j$ obtained after the operation is in $\{\mathbf{d}_i\}$ frame. The displacement gradient tensor for the configuration Ω_j referenced to Ω_{00} is given by $\nabla_{\Omega_{00}} \mathbf{u}_j$, where $\mathbf{u}_j = \mathbf{R}_j - \mathbf{R}_{00}$.

We are now in the position to elaborate on the fully-coupled Poisson's effect. For the deformed configuration Ω_2 , the strain vectors may be obtained using Eqs. (25) and (29), thus giving

$$\langle \boldsymbol{\lambda}_1^2, \mathbf{d}_1 \rangle = (\bar{\epsilon}_1 + \xi_3 \bar{\kappa}_2 - \xi_2 \bar{\kappa}_3 + W_{,\xi_1}). \tag{33}$$

Intuitively, $\langle \boldsymbol{\lambda}_1^2, \mathbf{d}_1 \rangle$ is the axial strain field across the cross-section due to midcurve axial strain, bending and warping. Therefore, we can write Eq. (26) as

$$\hat{\xi}_i = (1 - \nu(\bar{\epsilon}_1 + \xi_3 \bar{\kappa}_2 - \xi_2 \bar{\kappa}_3 + W_{,\xi_1})) \xi_i \text{ for } i = 2, 3. \tag{34}$$

The strain vectors for the final deformed state Ω_3 can be obtained using the expression of position vector in Eqs. (27) and (29) as

$$\begin{aligned} \boldsymbol{\lambda}_1^3 &= (\boldsymbol{\epsilon} + \hat{\xi}_3 \mathbf{d}_{3,\xi_1} + \hat{\xi}_2 \mathbf{d}_{2,\xi_1} + \hat{\xi}_{3,\xi_1} \mathbf{d}_3 + \hat{\xi}_{2,\xi_1} \mathbf{d}_2 + W_{,\xi_1} \mathbf{d}_1 + W \mathbf{d}_{1,\xi_1}) \\ &= \left(\overbrace{\frac{\bar{\epsilon}_1 = \langle \boldsymbol{\epsilon}, \mathbf{d}_1 \rangle}{(1 + e) \cos \gamma_{11} - 1}} + \hat{\xi}_3 \bar{\kappa}_2 - \hat{\xi}_2 \bar{\kappa}_3 + W_{,\xi_1} \right) \mathbf{d}_1 \\ &\quad + \left(\overbrace{\frac{\bar{\epsilon}_2 = \langle \boldsymbol{\epsilon}, \mathbf{d}_2 \rangle}{(1 + e) \sin \gamma_{12}} - \hat{\xi}_3 \bar{\kappa}_1 + \hat{\xi}_{2,\xi_1} + W \bar{\kappa}_3} \right) \mathbf{d}_2 \\ &\quad + \left(\overbrace{\frac{\bar{\epsilon}_3 = \langle \boldsymbol{\epsilon}, \mathbf{d}_3 \rangle}{(1 + e) \sin \gamma_{13}} + \hat{\xi}_2 \bar{\kappa}_1 + \hat{\xi}_{3,\xi_1} - W \bar{\kappa}_2} \right) \mathbf{d}_3; \end{aligned}$$

$$\boldsymbol{\lambda}_2^3 = W_{,\xi_2} \mathbf{d}_1 + (\hat{\xi}_{2,\xi_2} - 1) \mathbf{d}_2 + \hat{\xi}_{3,\xi_2} \mathbf{d}_3;$$

$$\boldsymbol{\lambda}_3^3 = W_{,\xi_3} \mathbf{d}_1 + \hat{\xi}_{2,\xi_3} \mathbf{d}_2 + (\hat{\xi}_{3,\xi_3} - 1) \mathbf{d}_3. \tag{35}$$

3.2. Physical interpretation of $\boldsymbol{\lambda}_i^j$

Consider an infinitesimal vector $d\xi_1 \mathbf{E}_1$ in the undeformed state Ω_{00} joining two material points $(\xi_2, \xi_3) \in \blacksquare_{00}(\xi_1)$ and $(\xi_2, \xi_3) \in \blacksquare_{00}(\xi_1 + d\xi_1)$. Similarly, consider an infinitesimal vector $d\xi_2 \mathbf{E}_2$ connecting two material points $(\xi_2, \xi_3) \in \blacksquare_{00}(\xi_1)$ and $(\xi_2 + d\xi_2, \xi_3) \in \blacksquare_{00}(\xi_1)$. Finally, consider an infinitesimal vector $d\xi_3 \mathbf{E}_3$ connecting two material points $(\xi_2, \xi_3) \in \blacksquare_{00}(\xi_1)$ and $(\xi_2, \xi_3 + d\xi_3) \in \blacksquare_{00}(\xi_1)$. These three vectors transform to the following in the deformed state Ω_j

$$\mathbf{F}_j(d\xi_i \mathbf{E}_i) = d\xi_i (\boldsymbol{\lambda}_i^j + \mathbf{d}_i) \text{ for } i = 1 - 3 \text{ and } j = 1 - 3. \tag{36}$$

The Einstein summation is suppressed in the above equation. The index i represent the infinitesimal vectors. Therefore, for a unit arc length element

$$\boldsymbol{\lambda}_1^j = \mathbf{F}_j \mathbf{E}_1 - \mathbf{d}_1. \tag{37}$$

For the unit vectors \mathbf{E}_2 and \mathbf{E}_3 , (along the direction of $d\xi_2 \mathbf{E}_2$ and $d\xi_3 \mathbf{E}_3$, respectively), we see that

$$\boldsymbol{\lambda}_2^j = \mathbf{F}_j \mathbf{E}_2 - \mathbf{d}_2; \quad \boldsymbol{\lambda}_3^j = \mathbf{F}_j \mathbf{E}_3 - \mathbf{d}_3. \tag{38}$$

Therefore, $\boldsymbol{\lambda}_i^j$ represents the strain vector in the deformed state Ω_j corresponding to the vector \mathbf{E}_i in the undeformed state Ω_{00} . The action of deformation gradient tensor on an infinitesimal vector $\mathbf{d}\mathbf{R}_{00}$ can be understood from Eq. (30). The vector $\mathbf{d}\mathbf{R}_{00}$ is subjected to rigid body rotation (the contribution due to \mathbf{Q} in Eq. (30)) and change in magnitude (the contribution due to $\boldsymbol{\lambda}_i^j \otimes \mathbf{E}_i$, sum implied over i). The outer product $\boldsymbol{\lambda}_i^j \otimes \mathbf{E}_i$ filters out the i^{th} component of the vector $\mathbf{d}\mathbf{R}_{00}$ (for each i) and strains it along the vector $\boldsymbol{\lambda}_i^j$.

3.3. Deformation of the unit vectors

It is insightful to observe the deformation of vectors \mathbf{E}_i (not necessarily at the centroid) with $i = 1 - 3$ in the deformed state Ω_3 . Consider the infinitesimal vectors $d\xi_1 \mathbf{E}_1$, $d\xi_2 \mathbf{E}_2$ and $d\xi_3 \mathbf{E}_3$ as described in Section 3.2. As explained before, the deformation gradient tensor maps an infinitesimal vector $\mathbf{d}\mathbf{R}_{00}$ to $\mathbf{d}\mathbf{R}_3$. One might wonder as to what the deformation of a unit length vectors \mathbf{E}_i , which is not infinitesimally small, means. The idea is that if the deformation gradient tensor deforms the vector, say $\mathbf{d}\mathbf{R}_{00} = d\xi_i \mathbf{E}_i \in T_p \Omega_{00}$ (no sum on i) to some vector $\mathbf{d}\mathbf{R}_3 \in T_{\phi_3(p)} \Omega_3$, then the vector $\mathbf{E}_i \in T_p \Omega_{00}$ deforms to $\frac{d\mathbf{R}_3}{d\xi_i} \in T_{\phi_3(p)} \Omega_3$. Mathematically, for a point $p \in \Omega_{00}$ the fact $\mathbf{F}_j(d\xi_1 \mathbf{E}_1) \in T_{\phi_j(p)} \Omega_j$ implies $\mathbf{F}_j \mathbf{E}_1 \in T_{\phi_j(p)} \Omega_j$ and $\mathbf{F}_j(d\xi_1 \mathbf{E}_1) \parallel \mathbf{F}_j \mathbf{E}_1$. One must understand that this deformation is different from the real deformed state of a finite length vector (which may be some curve!).

This idea of deformation of the unit vector or a unit arc length element is useful to understand the strain vectors and to interpret the contributions to the strain due to various finite strain parameters. Section [4.1] of Schutz (2009) is an excellent read on the idea of element in continuum mechanics.

3.3.1. Deformation of the unit vector \mathbf{E}_1

It is clear from Eqs. (35) and (37) that

$$\begin{aligned} \mathbf{F}_3 \mathbf{E}_1 &= \boldsymbol{\lambda}_1^3 + \mathbf{d}_1 \\ &= \left((1 + e) \cos \gamma_{11} + \hat{\xi}_3 \bar{\kappa}_2 - \hat{\xi}_2 \bar{\kappa}_3 + W_{,\xi_1} \right) \mathbf{d}_1 \\ &\quad + \left((1 + e) \sin \gamma_{12} - \hat{\xi}_3 \bar{\kappa}_1 + \hat{\xi}_{2,\xi_1} + W \bar{\kappa}_3 \right) \mathbf{d}_2 \\ &\quad + \left((1 + e) \sin \gamma_{13} + \hat{\xi}_2 \bar{\kappa}_1 + \hat{\xi}_{3,\xi_1} - W \bar{\kappa}_2 \right) \mathbf{d}_3; \end{aligned} \tag{39}$$

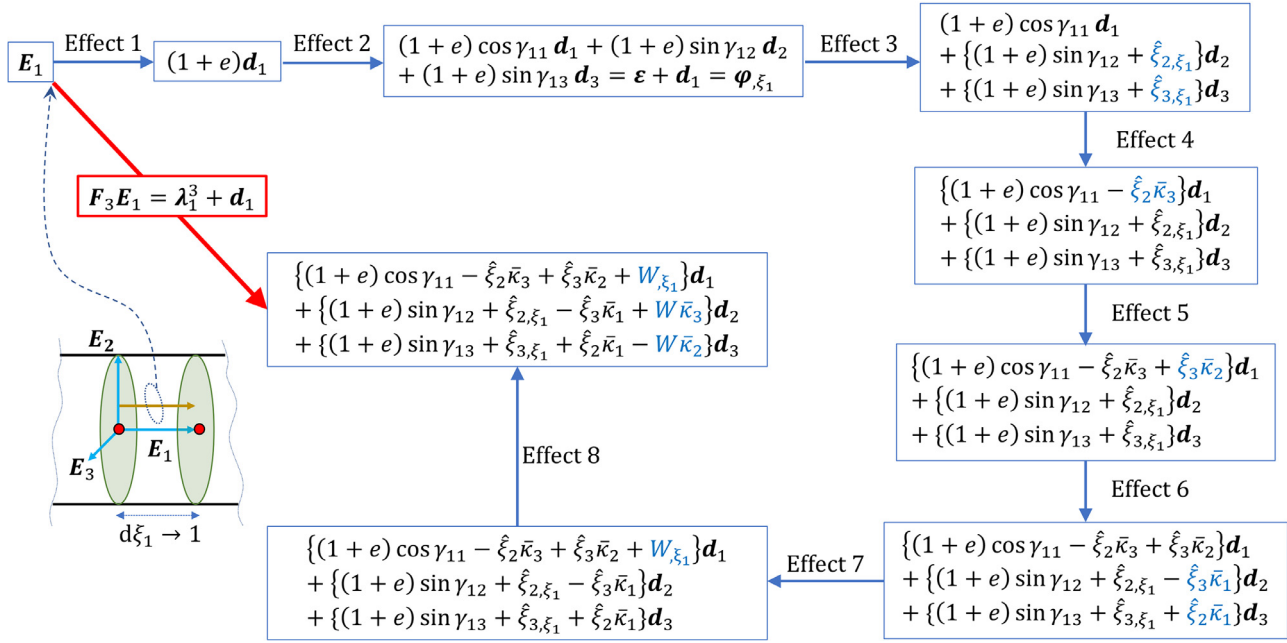


Fig. 3. Flowchart showing deformation of the unit vector E_1 in the configuration Ω_3 referenced to the configuration Ω_0 .

The Fig. 3 demonstrates straining of the vector E_1 (not necessarily along the midcurve). Each subsequent step in the flowchart does not represent superimposition; rather, each step represents the inclusion of various deformation effects, as indicated.

Certain points interpreting Fig. 3 are discussed below,

1. Fig. 3 is an improved version of Fig. 3 in Chadha and Todd (2017b). The transformation of the vector E_1 as shown in Fig. 3 considers the final deformed state as Ω_3 that incorporates fully-coupled Poisson's and warping effect.
2. Effects 1 and 2 represent the strain due to finite shear and midcurve axial deformation. Effect 1 is special case of effect 2, when there is no shear. The vector E_1 transforms to the vector $\epsilon + d_1$ if we consider effect 1 and 2 only.
3. Effect 3 addresses the strain in the vector E_1 for a unit arc length element ($d\xi_1 = 1$) due to differential Poisson's deformation. Fig. 4 gives a geometric description of effect 1 and 3.
4. Effects 4, 5 and 6 represent the strain due to bending and torsion about the vectors d_3 , d_2 and d_1 respectively. Unlike the description in Chadha and Todd (2017b) that utilizes the point (ξ_2, ξ_3) to define bending and torsion strains, we use $(\hat{\xi}_2, \hat{\xi}_3)$ to capture bending and torsion strains (notice the terms like $\hat{\xi}_2 \bar{\kappa}_1$, $\hat{\xi}_2 \bar{\kappa}_2$, $\hat{\xi}_2 \bar{\kappa}_3$ etc.). This is direct consequence of the fully-coupled Poisson's effect.
5. Effect 7 represents axial strain in E_1 due to differential warping deformation causing an additional axial strain of W_{ξ_1} along d_1 .
6. Effect 8 describes the strain $W d_{1,\xi_1} = W(\bar{\kappa}_3 d_2 - \bar{\kappa}_2 d_3)$. Note that effect 7 and 8 are obtained by realizing the strain contribution due to the quantity $(W d_1)_{,\xi_1}$. In effect 7, the director d_1 is kept constant but the change in the warping function is considered. Whereas, in effect 8, the warping deformation remains unchanged but the change in the orientation of director d_1 is considered (attributed to bending about d_2 and d_3). Fig. 5 describes effect 7 and 8.

3.3.2. Deformation of the unit vector E_2 (or E_3)

The deformation of the vector E_2 is explored considering the deformation of the cross-section $\blacksquare_{00}(\xi_1)$. Consider an infinitesimal vector $d\xi_2 E_2 \in \blacksquare_{00}(\xi_1)$ that deforms to $d\xi_2 (F_3 E_2)$ in the deformed

configuration Ω_3 . From Eqs. (35) and (38),

$$F_3 E_2 = \underbrace{W_{\xi_2} d_1}_{\text{Effect b}} + \underbrace{\hat{\xi}_2 d_2 + \hat{\xi}_3 d_3}_{\text{Effect a}} \quad (40)$$

It is observed that there are two effects that governs the deformation in this case. Effect *a* represents the straining in the vector $d\xi_2 E_2$ due to in-plane deformation of the cross-section from $\blacksquare_{00}(\xi_1) \rightarrow \blacksquare_3(\xi_1)$ attributed to the fully-coupled Poisson's transformation P_{ξ_1} . Effect *b* represents the straining due to the out of plane deformation of the cross-section attributed to warping. Fig. 6 illustrates the deformation of the vector E_2 .

It is clear from Eq. (30) that the deformation gradient tensor F_j in the deformed configuration Ω_j referenced to the undeformed state Ω_{00} can be obtained if the expression of λ_i^j is known (for $i = 1 - 3$). Appendix A.2 gives the expressions of λ_i^j for other deformed states.

3.4. Deformation gradient tensor of the deformed state referenced to the curved reference state

Consider that the curved reference beam configuration Ω_0 obtained by straining Ω_{00} such that the total length of the midcurve remains the same and there is no shear or torsion in the cross-sections. Consider an infinitesimal vector dR_{00} in the straight configuration Ω_{00} that transforms to dR_0 in the curved reference state Ω_0 such that from Eq. 29 of Chadha and Todd (2017b), we have

$$F_0 = \frac{dR_0}{dR_{00}} = \underbrace{\epsilon_0 \otimes E_1 + Q_0}_{\bar{\epsilon}_0}; \quad (41)$$

$$\epsilon_0 = (\hat{\xi}_3 \bar{\kappa}_{02} - \hat{\xi}_2 \bar{\kappa}_{03}) d_{01}.$$

The vector ϵ_0 represents the strain vector. The parameters $\bar{\kappa}_{02}(\xi_1)$ and $\bar{\kappa}_{03}(\xi_1)$ represents the finite bending curvature field for the curved reference state Ω_0 . Noting Eq. 32 and Eq. 35 from Chadha and Todd (2017b), we have

$$|F_0| = 1 + \langle \epsilon_0, d_{01} \rangle = 1 + \bar{\epsilon}_0; \quad (42a)$$

$$F_0^{-1} = Q_0^T \left[I_3 - \frac{1}{|F_0|} (\epsilon_0 \otimes d_{01}) \right]. \quad (42b)$$

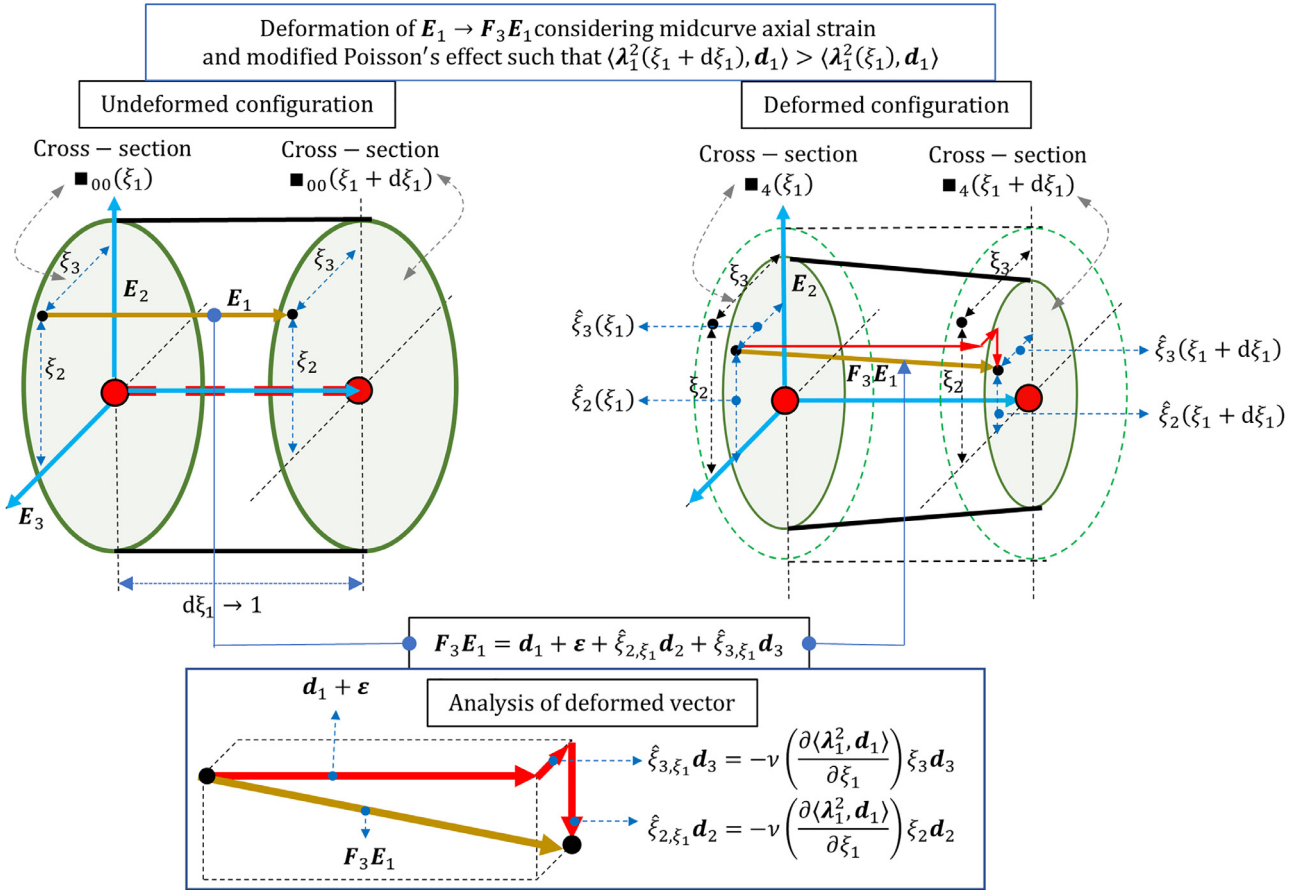


Fig. 4. Geometric description of effect 1 and 3:- deformation of vector E_1 considering differential Poisson's deformation in the cross section $\blacksquare_4(\xi_1)$ and $\blacksquare_4(\xi_1 + d\xi_1)$.

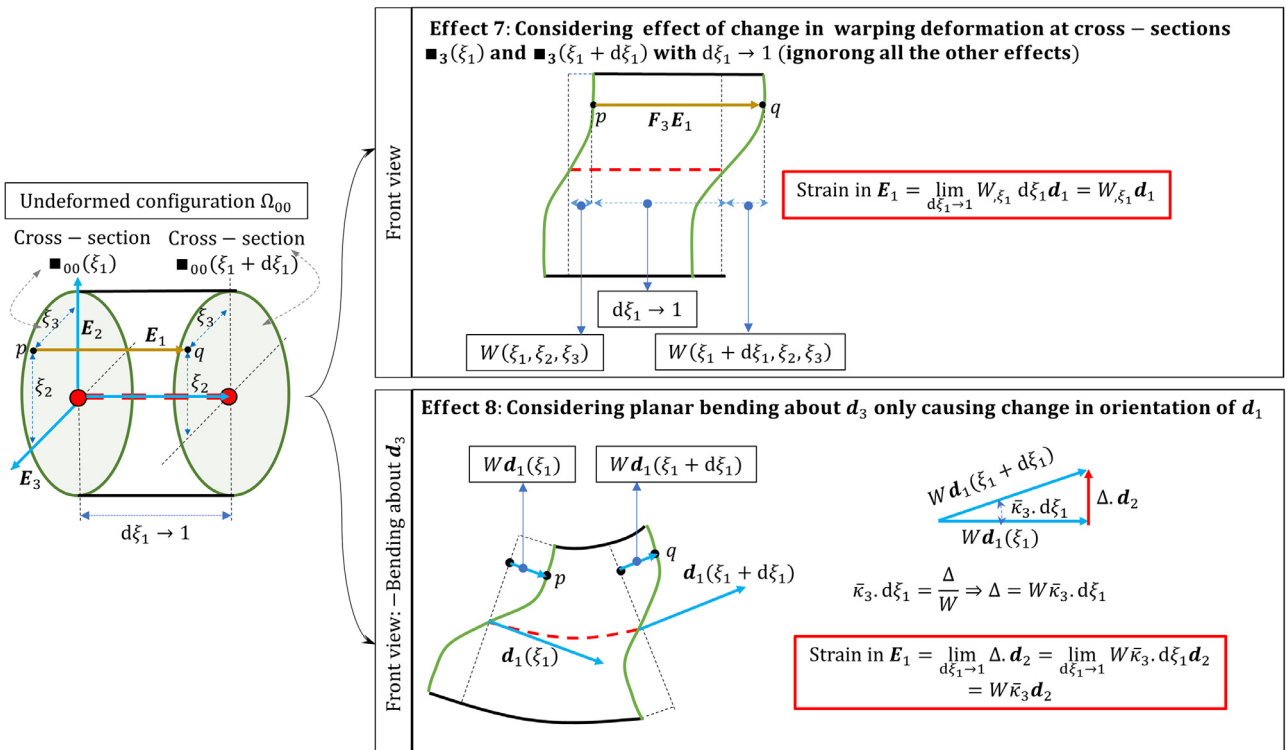


Fig. 5. Geometric description of effect 7 and 8.

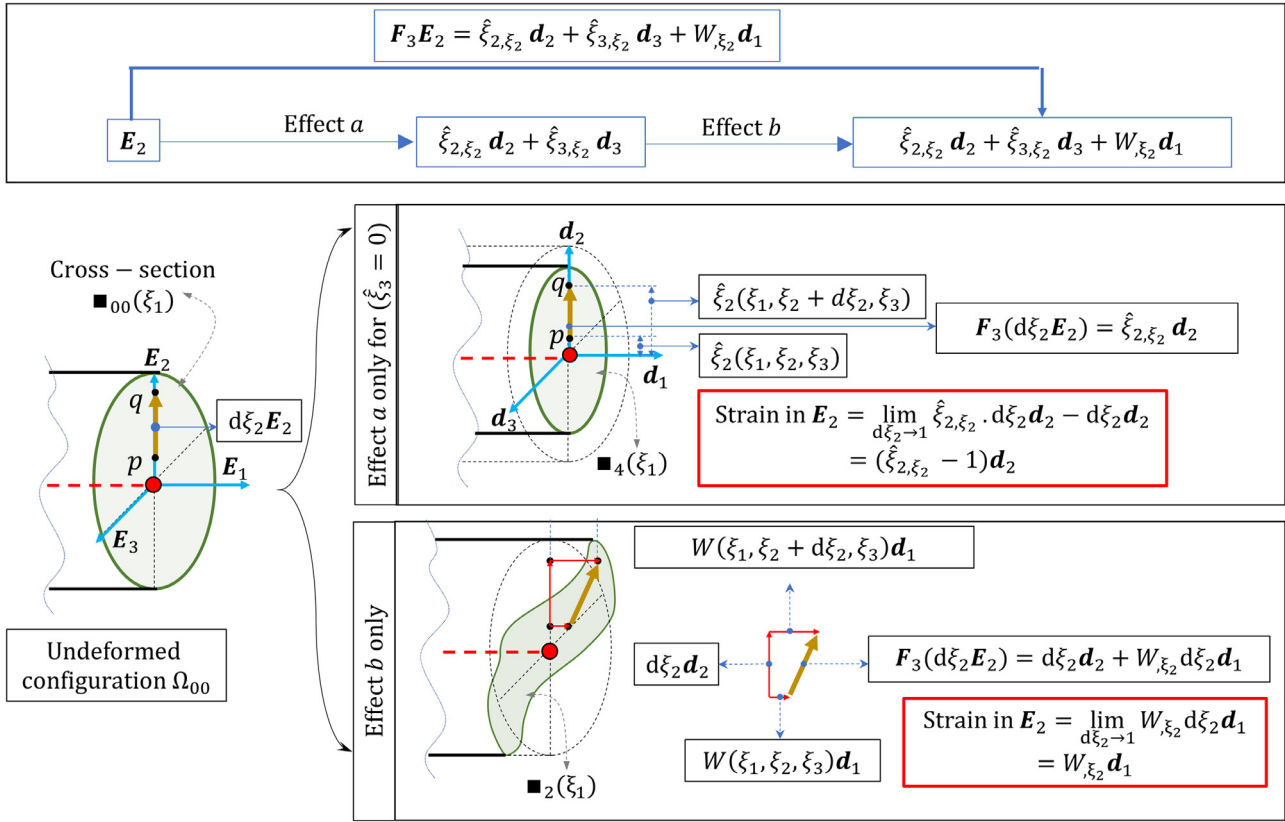


Fig. 6. Deformation of the infinitesimal vector $d\xi_2 E_2$.

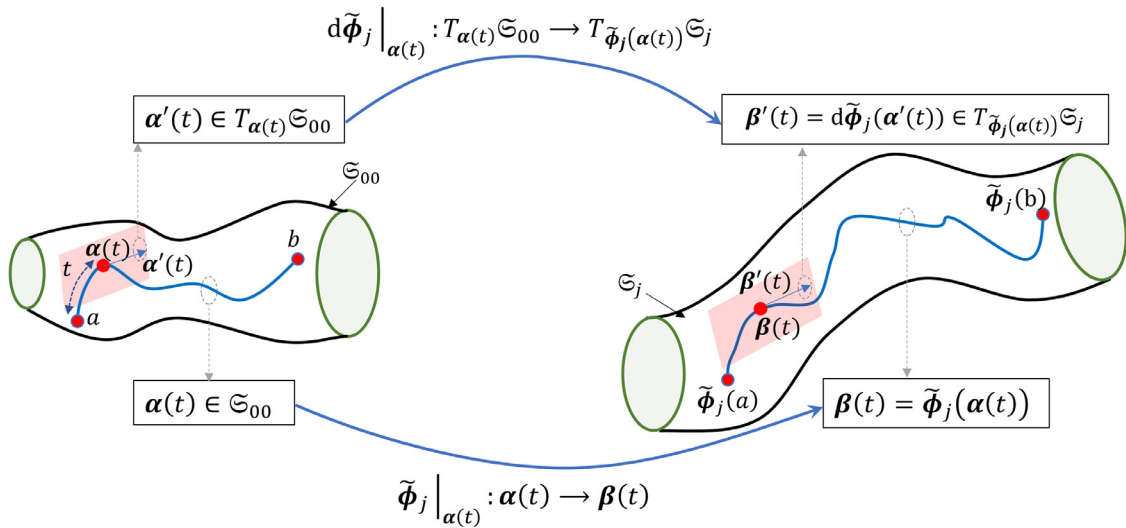


Fig. 7. Deformation of a finite length curve on the beam surface.

Here, $|F_0|$ represents the determinant of the tensor F_0 . For proof of the identity (42b) refer section 3.1.3 in Chadha and Todd (2017b). Note that the displacement gradient matrix $[\nabla_{\Omega_{00}} \mathbf{u}_0]_{d_{0i} \otimes E_m}$, with $\mathbf{u}_0 = \mathbf{R}_0 - \mathbf{R}_{00}$, has rank 1 and is nonsingular if $\epsilon_0 \neq 0$ (it is zero along the midcurve in the configuration Ω_0). This property allowed us to obtain Eq. (42b) using the result Eq. (1) in Miller Miller (1981). The deformation gradient tensor F_j^r of the deformed state Ω_j referenced to an initially curved (but unstrained) reference configuration Ω_0 can be obtained using the results mentioned above as

$$F_j^r = F_j F_0^{-1} = \left[(\lambda_i^j \otimes E_i) + Q \right] Q_0^T \left[I_3 - \frac{1}{|F_0|} (\epsilon_0 \otimes d_{0i}) \right]$$

$$= \left[(\lambda_i^j \otimes d_{0i}) + Q_r \right] - \left[\frac{\langle \epsilon_0, d_{0i} \rangle}{|F_0|} (\lambda_i^j \otimes d_{0i}) + \frac{1}{|F_0|} (Q_r \epsilon_0) \otimes d_{0i} \right] = (\lambda_i^j \otimes d_{0i}) + Q_r. \tag{43}$$

In the above equation, the relative strain vectors λ_i^{rj} are given as

$$\lambda_1^{rj} = \frac{1}{|F_0|} (\lambda_1^j - Q_r \epsilon_0); \quad \lambda_2^{rj} = \lambda_2^j; \quad \lambda_3^{rj} = \lambda_3^j. \tag{44}$$

In component form,

$$[F_{j pq}^r]_{d_p \otimes d_{0q}} = \langle \lambda_q^j, d_p \rangle + \delta_{pq}. \tag{45}$$

Physically, $\lambda_1^{r_j}$ represents the strain vector in the deformed state Ω_j corresponding to the vector \mathbf{d}_0 in the undeformed state Ω_0 .

Appendix A.3 elaborates the vector $\lambda_1^{r_j}$ for various deformed configurations Ω_j . Appendix A.4 discusses the procedure to obtain deformation gradient tensor of a deformed configuration with respect to another deformed state.

4. Measurement model for finite length and discrete strain gauge

4.1. On finite length strain gauge measurement

4.1.1. Geometric description of the deformation of finite strain gauge

Consider a strain gauge of finite length l_0 (not necessarily small) attached to the surface of beam \mathfrak{S}_{00} in the undeformed state Ω_{00} . Let $a \in \mathfrak{S}_{00}$ and $b \in \mathfrak{S}_{00}$ represent two ends of the finite strain gauge. Let us consider the unstrained segment of FBG sensor as a space curve $\alpha : [0, l_0] \rightarrow \mathfrak{S}_{00}$, with $\alpha(0) = a$ and $\alpha(l_0) = b$ such that

$$\alpha(t) = \xi_1(t)\mathbf{E}_1, \quad t \in [0, l_0], \quad (\xi_1, \xi_2, \xi_3) \in \mathfrak{S}_{00}. \tag{46}$$

The curve $\alpha(t)$ is parameterized by its arclength t . Therefore, $\alpha_{,t}(t) \in T_{\alpha(t)}\mathfrak{S}_{00}$ is a unit tangent vector along the curve. Here, $T_{\alpha(t)}\mathfrak{S}_{00}$ represents the tangent space of the manifold \mathfrak{S}_{00} restricted to the curve $\alpha(t)$. The curve $\alpha(t)$ maps to the curve $\check{\phi}_j(\alpha(t)) = \beta_j(t) : [0, l_0] \rightarrow \mathfrak{S}_j$, such that $\mathbf{F}_j\alpha_{,t}(t) = \beta_{j,t}(t) \in T_{\check{\phi}_j(\alpha(t))}\mathfrak{S}_j$. The vector field $\beta_{j,t}(t)$ is not a unit vector as t is not the arc length of the curve $\beta(t)$. The magnitude of the tangent vector $\beta_{j,t}(t)$ can be obtained as

$$\begin{aligned} |\beta_{j,t}(t)| &= \langle \beta_{j,t}(t), \beta_{j,t}(t) \rangle^{\frac{1}{2}} = \langle \mathbf{F}_j\alpha_{,t}(t), \mathbf{F}_j\alpha_{,t}(t) \rangle^{\frac{1}{2}} \\ &= \langle \alpha_{,t}(t), \mathbf{F}_j^T \mathbf{F}_j \alpha_{,t}(t) \rangle^{\frac{1}{2}} \\ &= \langle \alpha_{,t}(t), \mathbf{C}_j \alpha_{,t}(t) \rangle^{\frac{1}{2}} = \sqrt{C_{jpp} \alpha_{p,t} \alpha_{q,t}} \end{aligned} \tag{47}$$

Here, $\mathbf{C}_j = \mathbf{F}_j^T \mathbf{F}_j = \mathbf{U}_j^T \mathbf{U}_j$ represents the right Cauchy Green deformation tensor. In fact, the Cauchy Green deformation tensor can be thought as a push-forward Riemannian Metric (refer chapter 2 of Do Carmo (1992)) in the deformed configuration Ω_j (and the surface \mathfrak{S}_j as well). This is because for any pair of tangent vector $\mathbf{v}_1, \mathbf{v}_2 \in T_p\Omega_{00}$ (or $T_q\mathfrak{S}_{00}$), the tensor \mathbf{C}_j associates an inner product $\langle \mathbf{F}_j\mathbf{v}_1, \mathbf{F}_j\mathbf{v}_2 \rangle$ on the tangent space $T_{\check{\phi}_j(p)}\Omega_j$ (or $T_{\check{\phi}_j(q)}\mathfrak{S}_j$) such that $\mathbf{F}_j\mathbf{v}_1, \mathbf{F}_j\mathbf{v}_2 \in T_{\check{\phi}_j(p)}\Omega_j$ (or $T_{\check{\phi}_j(q)}\mathfrak{S}_j$). The length of the curve $\beta(t)$ as a function of the parameter t is obtained as

$$l_j(t) = \int_0^t |\beta_{j,t}(k)| dk = \int_0^t \sqrt{[C_{jpp} \alpha_{p,t} \alpha_{q,t}]_{(t=k)}} dk, \tag{48}$$

The scalar strain $\tilde{e}_j(t)$ at the material point $(\xi_1(t), \xi_2(t), \xi_3(t)) \in \Omega_j$ and the average scalar strain \tilde{e}_j^{avg} in the strain gauge is

$$\tilde{e}_j(t) = |\beta_{j,t}(t)| - 1; \tag{49}$$

$$\tilde{e}_j^{\text{avg}} = \frac{l_j(t=l_0)}{l_0} - 1.$$

4.1.2. Illustration

Consider a cantilever beam with circular cross-section of radius $r = 0.05$ m and length $l_0 = 1$ m. Let the finite length strain gauge join the material point $a = (0, 0, 0.05) \in \mathfrak{S}_{00}$ and $b = (1, 0, 0.05) \in \mathfrak{S}_{00}$ giving a straight curve $\alpha(t) = \xi_1(t)\mathbf{E}_1 + 0.05\mathbf{E}_3$ with $t \equiv \xi_1 \in [0, 1]$. Note that in this case $\xi_{1,t}(t) = 1$. Hence, $\alpha_{,t}(t) = \mathbf{E}_1$. Let the beam be subjected to the following finite strain parameters,

$$\bar{\kappa}_1(\xi_1) = 2\pi, \quad e(\xi_1) = 0.1, \quad \text{with } \nu = 0.3. \tag{50}$$

The deformed state for this example is Ω_3 with vanishing $\bar{\kappa}_2, \bar{\kappa}_3$ and W . It is intuitive that the curve $\alpha(t)$ deforms to $\beta_3(t) \in \mathfrak{S}_3$

(hence $j=3$) which is a helix with pitch length $l_p = (1 + e) = 1.1$ m, radius $r_1 = (1 - \nu)r$ and number of turn $n_{\text{turn}} = 1$. From the equation of length of helix, the length of the curve $\beta_3(t)$ can be obtained as,

$$l_2 = 2\pi n_{\text{turn}} \sqrt{r_1^2 + \left(\frac{l_p}{2\pi}\right)^2} = 1.141 \text{ m}; \tag{51}$$

$$\tilde{e}_3^{\text{avg}} = 14.1\%.$$

Now we obtain the length of the curve $\beta_3(t)$ using the discussion in previous section and the result (30). We have

$$\begin{aligned} \beta_{3,t} &= \mathbf{F}_3\alpha_{,t}(t) = \lambda_1^3(t) + \mathbf{d}_1 = (1 + e(\xi_1(t)))\mathbf{d}_1 \\ &\quad - \hat{\xi}_3(t)\bar{\kappa}_1(\xi_1(t))\mathbf{d}_2 + \hat{\xi}_2(t)\bar{\kappa}_1(\xi_1(t))\mathbf{d}_3. \end{aligned} \tag{52}$$

Since the undeformed curve (a mathematical equivalent of unstrained finite length strain gauge) is along \mathbf{E}_1 with $\xi_2 = 0$, we have $\hat{\xi}_2(t) = 0$ and $\hat{\xi}_3(t) = (1 - \nu)r$. Hence,

$$l_2 = \int_0^1 \langle \beta_{3,t}, \beta_{3,t} \rangle^{\frac{1}{2}} dt = \int_0^1 \sqrt{((1 + e)^2 + (1 - \nu)r\bar{\kappa}_1)^2} dt = 1.141 \text{ m}. \tag{53}$$

Thus, the results from Eqs. (51) and (53) are exactly the same.

4.2. On discrete ‘‘point’’ strain measurements

In strict sense, a discrete point strain gauge is an absurd idea because a point does not strain. In reality, a discrete strain gauge has a small but finite undeformed gage length associated with it. The discrete strain gauge with small gauge length can be treated by considering it as an infinitesimal vector such that its orientation in the undeformed state is known and gage length represents the length of the vector. This can help us estimate strain in average sense, by assuming that the finite strain parameters along the length of discrete strain gauge is constant throughout its length. We consider the value of the deformation gradient tensor at the center point of the strain gauge. Since the gauge length of discrete strain gauge is small and the finite strain parameters are continuous, this approach gives an excellent estimation of the scalar strain value.

4.2.1. Orientation of the surface strain gauge in the undeformed state Ω_{00}

Consider the undeformed configuration Ω_{00} that consist of continuously varying family of planar cross-sections $\blacksquare_{00}(\xi_1)$. Consider a strain gauge attached to the point $q_{00} = (\xi_1^g, \xi_2^g, \xi_3^g) \in \mathfrak{S}_{00}$ such that the unit direction vector $\mathbf{n}_{00} \in T_{q_{00}}\mathfrak{S}_{00}$. The strain gauge can be located from the point on the midcurve $p_{00} = (0, 0) \in \blacksquare_{00}(\xi_1^g)$ by the vector $\mathbf{r}_{00}^g = \xi_2^g\mathbf{E}_2 + \xi_3^g\mathbf{E}_3$. The tangent plane $T_{q_{00}}\mathfrak{S}_{00}$ is spanned by the unit orthonormal vectors $\mathbf{t}_{00}(\xi_1^g, \xi_2^g, \xi_3^g) - \tilde{\mathbf{t}}_{00}(\xi_1^g, \xi_2^g, \xi_3^g)$. The vector $\tilde{\mathbf{t}}_{00}$ lies in the plane spanned by $\mathbf{E}_1 - \mathbf{r}_{00}^g$, such that

$$\begin{aligned} \tilde{\mathbf{t}}_{00} &= \cos \tilde{\mu} \mathbf{E}_1 + \sin \tilde{\mu} \left(\frac{\mathbf{r}_{00}^g}{|\mathbf{r}_{00}^g|} \right) = \cos \tilde{\mu} \mathbf{E}_1 + \left(\frac{\xi_2^g \sin \tilde{\mu}}{\sqrt{\xi_2^{g2} + \xi_3^{g2}}} \right) \mathbf{E}_2 \\ &\quad + \left(\frac{\xi_3^g \sin \tilde{\mu}}{\sqrt{\xi_2^{g2} + \xi_3^{g2}}} \right) \mathbf{E}_3. \end{aligned} \tag{54}$$

The vector \mathbf{t}_{00} represents the unit tangent vector to the periphery Γ_{00} of the cross-section $\blacksquare_{00}(\xi_1^g)$, such that

$$\mathbf{t}_{00} = \mathbf{E}_1 \times \left(\frac{\mathbf{r}_{00}^g}{|\mathbf{r}_{00}^g|} \right) = - \left(\frac{\xi_3^g}{\sqrt{\xi_2^{g2} + \xi_3^{g2}}} \right) \mathbf{E}_2 + \left(\frac{\xi_2^g}{\sqrt{\xi_2^{g2} + \xi_3^{g2}}} \right) \mathbf{E}_3. \tag{55}$$

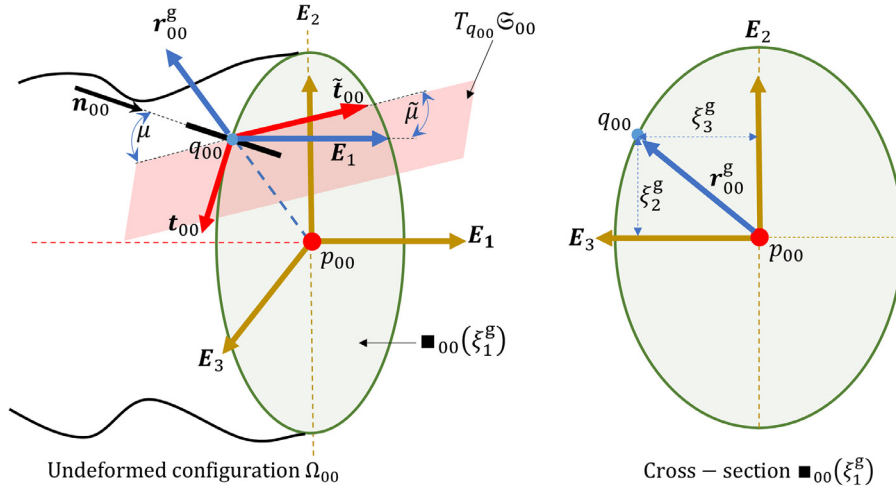


Fig. 8. Orientation of the strain gauge in undeformed configuration Ω_{00} .

The vector \mathbf{n}_{00} makes an angle μ with the vector $\tilde{\mathbf{t}}_{00}$ at the point q_{00} . Fig. 8 describes the orientation of the strain gauge in the undeformed state. The expression for \mathbf{n}_{00} is obtained as

$$\mathbf{n}_{00} = \cos \mu \tilde{\mathbf{t}}_{00} + \sin \mu \mathbf{t}_{00}. \quad (56)$$

If the configuration Ω_{00} consists of the same cross-sections (not varying along the beam), then $\tilde{\mu} = 0$.

As, $d\tilde{\boldsymbol{\phi}} : T_{q_{00}}\mathfrak{S}_{00} \rightarrow T_{\tilde{\boldsymbol{\phi}}(q_{00})}\mathfrak{S}_j$, the tangent space $T_{\tilde{\boldsymbol{\phi}}(q_{00})}\mathfrak{S}_j$ is spanned by the normal basis vectors $\left(\frac{\mathbf{F}_j \cdot \tilde{\mathbf{t}}_{00}}{|\mathbf{F}_j \cdot \tilde{\mathbf{t}}_{00}|}, \frac{\mathbf{F}_j \cdot \mathbf{t}_{00}}{|\mathbf{F}_j \cdot \mathbf{t}_{00}|} \right)$. These basis vectors are not orthogonal unless $\mathbf{F}_j = \mathbf{Q}$ at the point q_{00} .

4.2.2. Expression of scalar strain value of discrete strain gauge

Consider a discrete strain gauge with the finite (but small) gauge length l_g with the orientation \mathbf{n}_{00} in the undeformed state. Let the center point of the strain gauge be attached to the material point q_{00} . Considering the strain gauge as the vector $l_g \mathbf{n}_{00}$, the scalar strain \bar{e}_j in the deformed state Ω_j is,

$$\bar{e}_j = \overbrace{\langle \mathbf{F}_j(q_{00}) \mathbf{n}_{00}, \mathbf{F}_j(q_{00}) \mathbf{n}_{00} \rangle}^{\text{Stretch } \hat{\lambda}_j} - 1. \quad (57)$$

Eq. (57) defines *nominal strain*. We can obtain natural strain, Lagrangian strain, Eulerian strain, and logarithmic strain fields using the expression of stretch $\hat{\lambda}_j$ (refer to Section 4.2 of Asaro and Lubarda (2006)). Note that a similar expression can be obtained by using Eqs. (48) and (49) such that the deformation gradient tensor is assumed to be constant $\mathbf{F}_j(q_{00})$ (considering its value at the center of the strain gauge) along the length of the discrete strain gauge.

In Todd et al. (2013) and Chadha and Todd (2017a), the scalar strain was obtained using the expression (for $j = 1$ as the deformed state considered was Ω_1),

$$\bar{e}_1 = \langle \boldsymbol{\lambda}_1^1, \mathbf{n}_1 \rangle. \quad (58)$$

We assumed that the unit direction vector \mathbf{n}_{00} transforms to the unit vector $\mathbf{n}_1 = \mathbf{Q} \mathbf{n}_{00}$. Eq. (58) captures bending and axial strains in the same sense as Eq. (57) but it fails to capture finite strains due to multiple deformation effects. The result obtained from Eq. (58) also depends on the orientation of the strain gauge \mathbf{n}_{00} . For instance, consider a discrete strain gauge with finite length attached to beam along the direction $\mathbf{n}_{00} = \mathbf{E}_1$ such that the center of the strain gauge is at point q_{00} . Suppose that the beam has circular cross-section and is subjected to pure torsion with curvature

field $\bar{\kappa}_1(\xi_1)$. From Eq. (57), the scalar strain in the strain gauge will be,

$$\bar{e}_1 = \sqrt{1 + r_g^2 \bar{\kappa}_1^2(\xi_1^g)} - 1 = \frac{r_g^2 \bar{\kappa}_1^2(\xi_1^g)}{2} - \frac{r_g^4 \bar{\kappa}_1^4(\xi_1^g)}{8} + O[\kappa_1^5]. \quad (59)$$

Where, $r_g = \sqrt{\xi_2^g + \xi_3^g}$. If we use Eq. (57) with $\mathbf{n}_1 = \mathbf{Q} \mathbf{E}_1 = \mathbf{d}_1$, it is clear that the estimated scalar strain is zero. But this is not true because an infinitesimal vector along \mathbf{E}_1 will be strained due to torsion. Therefore, Eq. (57) represents the corrected version of Eq. (58). In fact, Eq. (58) worked well in Todd et al. (2013) as bending and axial strains were the only deformation effects considered, whereas in Chadha and Todd (2017a), the problem considered belonged to the class of large deformation but small strain with dominant cause of strain being bending and axial deformation.

5. Summary and conclusions

This paper can be divided into three broad domains. The first domain addresses the coupling between Poisson's and warping effect and obtaining a fully-coupled Poisson's transformation with the aim of developing a comprehensive kinematics of Cosserat beams. The kinematics developed is not restricted to the Euler-Bernoulli rigid cross-section assumption, and it is simultaneously maintaining the single manifold nature of the problem. The idea of having prior knowledge of the cross-sectional dependence of the warping function (function of the form $\Psi(\xi_2, \xi_3)$) is certainly desirable for maintaining the single manifold nature of the kinematics, but it yields only an approximate solution. The primary reason to investigate the coupling between Poisson's and warping effect (along with contribution to warping due to torsional and bending induced shear) and develop a fully-coupled Poisson's transformation, is to further refine the kinematics of the Cosserat beam model. This is beneficial for both forward modeling analyses and solving inverse problems like shape reconstruction from strain measurements.

We detail three different deformed configurations of the beam with Ω_3 representing the most general configuration and $\Omega_1 - \Omega_2$ representing more constrained cases. The coupled Poisson's and warping is developed in a two-stage process. We arrive at the governing differential equations to capture warping in an asymmetric beam cross-section subjected to curvatures and axial strains for the linear elastic case. The inclusion of axial strain and Poisson's effect in the small displacement field leads to an *inconsistent governing*

differential equation for warping (Eqs. (61a) and (61b)). We obtain the consistent differential equation (Eqs. (68a) and (68b)) by deliberately enforcing the inconsistency condition (Eqs. (65) and (66)) into the inconsistent warping equation. The consistent warping equation suggests a solution to the warping function W that is not explicitly dependent on the axial strain $e(\xi_1)$ and its derivatives. However, we carefully note that the elimination of inconsistency results in consistent differential equations for warping that could be solved, but the accuracy of the solution and their closeness to the exact 3D solution is open to further investigation. Motivated from the work of Burgoyne and Brown (1994) and Brown and Burgoyne (1994), we delineated two possible solution approaches to obtain the warping function in variable separable form. Stage one represents the incorporation of the effects of axial strains and Poisson's transformation on warping. The details of first stage of coupling are mentioned in Appendix A.1. In stage two, we propose the fully-coupled Poisson's transformation by considering the axial strain contributions due to midcurve strain, finite shear, bending curvatures, and out of plane warping. This yields fully coupled Poisson's and warping effect. We note that the proposed Poisson's transformation governing the in-plane deformation does not include the deformation due to local buckling, which is a prominent phenomenon in thin walled beams. However, the kinematic framework developed is completely general.

The second domain of investigation in this work develops the kinematics of the beam that includes fully-coupled Poisson's and warping effect along with finite curvatures, finite shear, and mid-curve axial strains. The deformation gradient tensor and strain vector in a general deformed state Ω_j referenced to both a mathematically straight beam configuration Ω_{00} and an initially curved reference configuration Ω_0 are derived. The contribution to deformation due to various effects are carefully explored and explained.

The third domain of this exposition exploits the results developed in the first half of the paper to investigate the mechanics of discrete and finite length strain gauges. We arrive at the expression of the scalar strain value that would be observed in strain gauges perfectly attached to the surface (or embedded into the beam) of Cosserat beam in terms of finite strain parameters and illustrate a simple example to validate our results. We critically review the formula of scalar surface strain that was proposed in our previous work on shape sensing (for finite deformation but small strain problem) and compare it to the expression arrived at this work.

In a much broader sense, this paper studies the differential geometry of the Cosserat beam. The results developed here will be used to extend our work on shape reconstruction that utilize local differential geometric parameters (finite strain parameters) to predict the global deformed state of the structure. The results in this paper establishes a relationship between the finite strain parameters and the measurement of a (perfectly affixed) strain gauge. This development may be used to estimate finite strain fields of the beam using a countable number of surface strain gauge. Furthermore, we can arrive at the deformation adaptive shape functions to develop FEM formulation of the beam more accurately.

Acknowledgements

Funding for this work was provided by the U.S. Army Corps of Engineers through the U.S. Army Engineer Research and Development Center Research Cooperative Agreement W912HZ-17-2-0024. We also gratefully thank Professor Elham Izadi, Department of Mathematics, UCSD for her valuable discussions on differential geometry.

Appendix A

A1. Inconsistencies in the governing differential equation of warping and the associated challenges

A1.1. Preliminary results

Before we present a deeper discussion, we note the following results. From the definition of t and \tilde{t} as in Eq. (22b), we have

$$\oint td\Gamma = \oint \langle [(\xi_2 E_2 + \xi_3 E_3) \times \mathbf{n}], E_1 \rangle d\Gamma = \oint \langle \mathbf{n}, (-\xi_3 E_2 + \xi_2 E_3) \rangle d\Gamma = \int_{\blacksquare} \text{Div}(-\xi_3 E_2 + \xi_2 E_3) d\xi_2 d\xi_3 = 0; \tag{60a}$$

$$\oint \tilde{t}d\Gamma = \oint \langle \mathbf{n}, (\xi_2 E_2 + \xi_3 E_3) \rangle d\Gamma = \int_{\blacksquare} \text{Div}(\xi_2 E_2 + \xi_3 E_3) d\xi_2 d\xi_3 = 2A(\xi_1); \tag{60b}$$

$$\int_{\blacksquare} \nabla^2 W d\xi_2 d\xi_3 = \oint W_{,n} d\Gamma. \tag{60c}$$

From here on, we will represent the area of the cross-section $A(\xi_1)$ as A . Eq. (60c) is obtained using the Gauss-divergence theorem. Recalling the governing differential equation for warping (22a) and (22b),

$$\nabla^2 W + \frac{\tilde{\lambda}}{G} (W_{,\xi_1 \xi_1} - \xi_2 \bar{\kappa}_{3,\xi_1} + \xi_3 \bar{\kappa}_{2,\xi_1}) + \bar{\lambda} e_{,\xi_1} = 0 \text{ on } \blacksquare(\xi_1); \tag{61a}$$

$$W_{,n} = -\bar{\kappa}_1 t + e_{,\xi_1} v \tilde{t} \text{ on } \Gamma(\xi_1). \tag{61b}$$

A1.2. The inconsistency

Integrating Eq. (61b) along the boundary of the cross-section $\Gamma(\xi_1)$ and using the result (60a) and (60b), we have

$$\oint W_{,n} d\Gamma = -\bar{\kappa}_1 \oint td\Gamma + e_{,\xi_1} v \oint \tilde{t}d\Gamma = 2vAe_{,\xi_1}. \tag{62}$$

Integrating Eq. (61a) across the cross-section $\blacksquare(\xi_1)$ and realizing that $\int_{\blacksquare} \xi_i d\xi_2 d\xi_3 = 0$ for $i = 2$ and 3 , we have

$$\int_{\blacksquare} \nabla^2 W d\xi_2 d\xi_3 = -\frac{\tilde{\lambda}}{G} \int_{\blacksquare} W_{,\xi_1 \xi_1} d\xi_2 d\xi_3 - \bar{\lambda} Ae_{,\xi_1}. \tag{63}$$

Using Eqs. (60c) and (63), we have

$$\oint W_{,n} d\Gamma = -\frac{\tilde{\lambda}}{G} \int_{\blacksquare} W_{,\xi_1 \xi_1} d\xi_2 d\xi_3 - \bar{\lambda} Ae_{,\xi_1}. \tag{64}$$

Comparing Eqs. (62) and (64), we clearly observe an inconsistency which can be resolved only if

$$\int_{\blacksquare} W_{,\xi_1 \xi_1} d\xi_2 d\xi_3 = -\left(\frac{GA(\xi_1)(\bar{\lambda} + 2v)}{\tilde{\lambda}}\right) e_{,\xi_1} = -\left(\frac{\tilde{\lambda} - 2v\lambda}{\tilde{\lambda}}\right) A(\xi_1) e_{,\xi_1}. \tag{65}$$

From the definition of the reduced axial force field $P_1(\xi_1)$ in Eq. (23), we obtain the following result

$$P_{1,\xi_1} = (\tilde{\lambda} - 2v\lambda)Ae_{,\xi_1} + \tilde{\lambda} \int_{\blacksquare} W_{,\xi_1 \xi_1} d\xi_2 d\xi_3 \tag{66}$$

The inconsistency condition (65) and the Eq. (66) implies that the inconsistency can be resolved if

$$P_{1,\xi_1} = 0 \text{ or } P_1(\xi_1) = \text{Constant} \tag{67}$$

These kind of inconsistencies or anomalies are commonly observed in simplified theories. For instance, the anomaly of the torque for the case of wholly-restrained end warping was observed by

Burgoyne and Brown (1994). If the axial strain and the Poisson's effect is not included in the displacement field (20), it would require $\int_{\square} W_{,\xi_1\xi_1} d\xi_2 d\xi_3 = 0$. This condition is automatically satisfied if $P_1 = 0$ along the length of the beam, which is physically true if axial deformation and force is ignored as in Eq. (7) of Brown and Burgoyne (1994). At the most fundamental level, the reason of this inconsistency lies primarily in our objective to obtain a simplified warping function and our assumption of zero body force. In our opinion, the inconsistency indicates that the rigid body cross-sectional deformation due to constant axial strain field across the cross-section attributed to midcurve axial strain $e(\xi_1)$ does not affect warping (essentially an out-of-plane deformation), which is clearly observed in Eqs. (79) and (96).

A1.3. Proposed solution to eliminate the inconsistency condition and obtain the warping function

We attempt to resolve the inconsistency by enforcing the condition (65) in the inconsistent warping equation. Substituting for $e_{,\xi_1}$ (obtained using Eq. (65)) in Eqs. (61a) and (61b), we obtain the modified consistent governing differential equation

$$\nabla^2 W + C_1(W_{,\xi_1\xi_1} - \xi_2 \bar{\kappa}_3 \xi_1 + \xi_3 \bar{\kappa}_2 \xi_1) + C_2 \bar{\lambda} \int_{\square} W_{,\xi_1\xi_1} d\xi_2 d\xi_3 = 0 \text{ on } \blacksquare(\xi_1), \tag{68a}$$

$$W_{,n} = -\bar{\kappa}_1 t + \left\{ \nu C_2 \int_{\square} W_{,\xi_1\xi_1} d\xi_2 d\xi_3 \right\} \tilde{t} \text{ on } \Gamma(\xi_1), \tag{68b}$$

where

$$C_1 = \frac{\tilde{\lambda}}{G} \text{ and } C_2 = -\frac{1}{A} \left(\frac{\tilde{\lambda}}{\tilde{\lambda} - 2\nu\lambda} \right). \tag{69}$$

A1.4. Solution approach 1: Solution of warping function using series sum

We assume a solution of the variable separable form

$$W(\xi_1, \xi_2, \xi_3) = \sum_{r=0}^{\infty} (\bar{\kappa}_1^{(r)} \Psi_{1r} + \bar{\kappa}_2^{(r)} \Psi_{2r} + \bar{\kappa}_3^{(r)} \Psi_{3r} + e^{(r)} \Psi_{4r}) \tag{70}$$

and aim at obtaining the functions Ψ_{ir} , where $i = 1 - 4$. Substituting Eq. (70) into the consistent differential Eqs. (68a) and (68b), we can obtain the governing differential equations for the functions Ψ_{ir} with $i = 1 - 4$.

The governing differential equations for the functions Ψ_{1r} :

For $r = 0$ and 1,

$$\nabla^2 \Psi_{10} = 0 \text{ on } \blacksquare(\xi_1) \text{ with } \Psi_{10,n} = -t \text{ on } \Gamma(\xi_1); \tag{71}$$

$$\nabla^2 \Psi_{11} = 0 \text{ on } \blacksquare(\xi_1) \text{ with } \Psi_{11,n} = 0 \text{ on } \Gamma(\xi_1);$$

For $r \geq 2$,

$$\nabla^2 \Psi_{1r} = -\left[C_1 \Psi_{1(r-2)} + \bar{\lambda} C_2 \int_{\square} \Psi_{1(r-2)} d\xi_2 d\xi_3 \right] \text{ on } \blacksquare(\xi_1);$$

$$\Psi_{1r,n} = \left[\nu C_2 \int_{\square} \Psi_{1(r-2)} d\xi_2 d\xi_3 \right] \tilde{t} \text{ on } \Gamma(\xi_1). \tag{72}$$

From Eq. (71), we note that Ψ_{11} is constant. To avoid any rigid body motion of the cross-section due to warping, we take $\Psi_{11} = 0$. Eq. (72) then implies $\Psi_{1r} = 0$ for any odd r .

If the cross-section is symmetric, $\int_{\square} \Psi_{10} d\xi_2 d\xi_3 = 0$ as Ψ_{10} is anti-symmetric. This reduces the governing differential equation for Ψ_{1r} for any even $r = 2, 4, 6, \dots$ to,

$$\nabla^2 \Psi_{1r} = -C_1 \Psi_{1(r-2)} \text{ on } \blacksquare(\xi_1) \text{ with } \Psi_{1r,n} = 0 \text{ on } \Gamma(\xi_1);$$

It is easy to prove then that $\int_{\square} \Psi_{1r} = 0$ for any even $r = 2, 4, 6, \dots$ implying that the non-trivial solution to the functions Ψ_{1r} is anti-symmetric. Thus, we observe that the anti-symmetric nature of the

solution (contribution to warping due to torsion) for the symmetric cross-section is preserved.

The governing differential equations for the functions Ψ_{2r} :

For $r = 0$ and 1,

$$\nabla^2 \Psi_{20} = 0 \text{ on } \blacksquare(\xi_1) \text{ with } \Psi_{20,n} = 0 \text{ on } \Gamma(\xi_1); \tag{73}$$

$$\nabla^2 \Psi_{21} = -C_1 \xi_3 \text{ on } \blacksquare(\xi_1) \text{ with } \Psi_{21,n} = 0 \text{ on } \Gamma(\xi_1).$$

For $r \geq 2$,

$$\nabla^2 \Psi_{2r} = -\left[C_1 \Psi_{2(r-2)} + \bar{\lambda} C_2 \int_{\square} \Psi_{2(r-2)} d\xi_2 d\xi_3 \right] \text{ on } \blacksquare(\xi_1);$$

$$\Psi_{2r,n} = \left[\nu C_2 \int_{\square} \Psi_{2(r-2)} d\xi_2 d\xi_3 \right] \tilde{t} \text{ on } \Gamma(\xi_1). \tag{74}$$

The governing differential equations for the functions Ψ_{3r} :

For $r = 0$ and 1,

$$\nabla^2 \Psi_{30} = 0 \text{ on } \blacksquare(\xi_1) \text{ with } \Psi_{30,n} = 0 \text{ on } \Gamma(\xi_1); \tag{75}$$

$$\nabla^2 \Psi_{31} = C_1 \xi_2 \text{ on } \blacksquare(\xi_1) \text{ with } \Psi_{31,n} = 0 \text{ on } \Gamma(\xi_1).$$

For $r \geq 2$,

$$\nabla^2 \Psi_{3r} = -\left[C_1 \Psi_{3(r-2)} + \bar{\lambda} C_2 \int_{\square} \Psi_{3(r-2)} d\xi_2 d\xi_3 \right] \text{ on } \blacksquare(\xi_1); \tag{76}$$

$$\Psi_{3r,n} = \left[\nu C_2 \int_{\square} \Psi_{3(r-2)} d\xi_2 d\xi_3 \right] \tilde{t} \text{ on } \Gamma(\xi_1).$$

Following similar reasoning as before, we observe from Eqs. (74) and (76) that $\Psi_{20} = 0$ and $\Psi_{30} = 0$. That implies, $\Psi_{2r} = 0$ and $\Psi_{3r} = 0$ for any even r . The inclusion of bending curvature in warping results in a non-linear strain profile across the cross-section.

The governing differential equations for the functions Ψ_{4r} :

For $r = 0$ and 1,

$$\nabla^2 \Psi_{40} = 0 \text{ on } \blacksquare(\xi_1) \text{ with } \Psi_{40,n} = 0 \text{ on } \Gamma(\xi_1); \tag{77}$$

$$\nabla^2 \Psi_{41} = 0 \text{ on } \blacksquare(\xi_1) \text{ with } \Psi_{41,n} = 0 \text{ on } \Gamma(\xi_1).$$

For $r \geq 2$,

$$\nabla^2 \Psi_{4r} = -\left[C_1 \Psi_{4(r-2)} + \bar{\lambda} C_2 \int_{\square} \Psi_{4(r-2)} d\xi_2 d\xi_3 \right] \text{ on } \blacksquare(\xi_1);$$

$$\Psi_{4r,n} = \left[\nu C_2 \int_{\square} \Psi_{4(r-2)} d\xi_2 d\xi_3 \right] \tilde{t} \text{ on } \Gamma(\xi_1). \tag{78}$$

Eq. (77) implies $\Psi_{40} = 0$ and $\Psi_{41} = 0$. This result coupled with the Eq. (78) results in $\Psi_{4r} = 0$ for any r . This result eliminates the explicit contribution to warping due to axial strain. Hence, we are left with a solution of the form

$$W(\xi_1, \xi_2, \xi_3) = (\bar{\kappa}_1 \Psi_{10} + \bar{\kappa}_1^{(2)} \Psi_{12} + \bar{\kappa}_1^{(4)} \Psi_{14} + \dots) + (\bar{\kappa}_2^{(1)} \Psi_{21} + \bar{\kappa}_2^{(3)} \Psi_{23} + \bar{\kappa}_2^{(5)} \Psi_{25} + \dots) + (\bar{\kappa}_3^{(1)} \Psi_{31} + \bar{\kappa}_3^{(3)} \Psi_{33} + \bar{\kappa}_3^{(5)} \Psi_{35} + \dots). \tag{79}$$

A1.5. Physical interpretation of the warping function Ψ_{31} (or Ψ_{21})

Claim: The warping contribution $\bar{\kappa}_3^{(1)} \Psi_{31}$ represents the out-of-plane deformation of the cross-section due a non-uniform shear stress field induced by bending about E_3 . This implies that the slope $\bar{\kappa}_3^{(1)} \frac{\partial \Psi_{31}}{\partial \xi_2}$ is the shear strain profile of the cross-section.

Proof. The warping is dependent on the geometry of the cross section. Therefore, let us consider a rectangular prismatic beam with the depth d and breadth b to proceed with further discussion.

For the proof, we assume that the claim is true and arrive at the governing equation for Ψ_{31} as in Eq. (75). If $M(\xi_1)$ and $V(\xi_1)$ represent the cross-sectional bending moment (about E_3) and shear respectively, then we know from the theory of bending that $V = \frac{dM}{d\xi_1}$ and $M = \bar{\kappa}_3 E I_{33}$, where $I_{33} = \frac{1}{12} b d^3$ is the moment of inertia about E_3 axis. The expression for the shear strain profile of rectangular section is given as

$$\gamma_{12} = \frac{6V}{Gbd^3} \left(\frac{d^2}{4} - \xi_2^2 \right) = \frac{6EI_{33}\bar{\kappa}_3^{(1)}}{Gbd^3} \left(\frac{d^2}{4} - \xi_2^2 \right). \tag{80}$$

Note that Poisson’s effect is ignored in traditional beam theory limiting the constant $C_1 = \frac{E}{G}$ (in Eq. (69)). Substituting for I_{33} and C_1 , the shear strain profile reduces to

$$\gamma_{12} = \frac{C_1 \bar{\kappa}_3^{(1)}}{2} \left(\frac{d^2}{4} - \xi_2^2 \right). \tag{81}$$

From our claim,

$$\begin{aligned} \bar{\kappa}_3^{(1)} \frac{\partial \Psi_{31}}{\partial \xi_2} &= \gamma_{12}; \\ \frac{\partial \Psi_{31}}{\partial \xi_2} &= \frac{C_1}{2} \left(\frac{d^2}{4} - \xi_2^2 \right). \end{aligned} \tag{82}$$

Taking the derivative with ξ_2 , and noting that γ_{12} is not a function of ξ_3 (implying $\frac{\partial^2 \Psi_{31}}{\partial \xi_2^2} = 0$), we can write

$$\nabla^2 \Psi_{31} = -C_1 \xi_2 \text{ on } \blacksquare(\xi_1). \tag{83}$$

We also note that for bending about \mathbf{E}_3 , we have $\frac{\partial \Psi_{31}}{\partial \xi_2} \Big|_{\xi_2 = \frac{d}{2}} = 0$ and $\frac{\partial \Psi_{31}}{\partial \xi_3} = 0$ (because Ψ_{31} does not have ξ_3 dependence), implying

$$\Psi_{31,n} = 0 \text{ on } \Gamma(\xi_1). \tag{84}$$

This completes the proof. \square

Further Comment:

Timoshenko’s beam theory assumes plane cross-section remains plane after deformation but relaxes the restriction of cross-section remaining perpendicular to the neutral surface. Thus assuming constant shear strain of $\gamma_{12} = \frac{1.5V}{Gbd} = 1.5 \frac{E}{G} \left(\frac{d^2}{4} \right)$ for a rectangular section with a shear coefficient 1.5. This leads us to define an equivalent warping function that incorporates Timoshenko shear deformation as

$$\begin{aligned} \Psi_{31}^t &= \frac{E}{2G} \left(\frac{d^2}{4} \xi_2 \right); \\ \Psi_{21}^t &= \frac{E}{2G} \left(\frac{d^2}{4} \xi_3 \right); \end{aligned} \tag{85}$$

such that if $v(\xi_1)$ and $w(\xi_1)$ represent total transverse displacement (including shear and bending) of the midcurve in \mathbf{E}_2 and \mathbf{E}_3 respectively and $\theta_2(\xi_1)$ and $\theta_3(\xi_1)$ represents bending rotations about the axes \mathbf{E}_2 and \mathbf{E}_3 , respectively, then

$$\frac{\partial v}{\partial \xi_1} - \theta_3 = \bar{\kappa}_3^{(1)} \Psi_{31,t,\xi_2} \tag{86}$$

$$\frac{\partial w}{\partial \xi_1} + \theta_2 = \bar{\kappa}_2^{(1)} \Psi_{21,t,\xi_3}.$$

Using Eq. (82) and the fact that $\Psi_{31}(0, 0) = \Psi_{21}(0, 0) = 0$, the warping functions Ψ_{31} (or Ψ_{21}) are obtained as,

$$\begin{aligned} \Psi_{31} &= \frac{E}{2G} \left(\frac{d^2}{4} \xi_2 - \frac{\xi_2^3}{3} \right) = \Psi_{31}^t - \frac{E}{2G} \left(\frac{\xi_2^3}{3} \right); \\ \Psi_{21} &= \frac{E}{2G} \left(\frac{d^2}{4} \xi_3 - \frac{\xi_3^3}{3} \right) = \Psi_{21}^t - \frac{E}{2G} \left(\frac{\xi_3^3}{3} \right). \end{aligned} \tag{87}$$

Fig. A.9 illustrates the discussion here.

A1.6. A practically useful warping function for large deformation

From the previous discussion, its clear that Ψ_{21}^t and Ψ_{31}^t are the linear part of the warping function Ψ_{21} and Ψ_{31} respectively. The displacement field assumed in (20) does not have shear deformation added explicitly. However, the inclusion of the warping component $\bar{\kappa}_3^{(1)} \Psi_{31}$ and $\bar{\kappa}_2^{(1)} \Psi_{21}$ generalizes the shear deformation assumed by Timoshenko to include out of plane bending-induced shear warping. Therefore, we should be careful in using

this general warping solution if the shear deformations are explicitly added. Since the kinematics developed in this paper includes finite shear, we propose a simplified warping function for the large deformation problem as

$$W(\xi_1, \xi_2, \xi_3) = \bar{\kappa}_1(\xi_1) \Psi_{10} + \bar{\kappa}_2^{(1)} (\Psi_{21} - \Psi_{21}^t) + \bar{\kappa}_3^{(1)} (\Psi_{31} - \Psi_{31}^t). \tag{88}$$

Secondly, an alternative warping function that can be defined as an improved version of warping used by Simo and Vu-Quoc (1991) (as defined by Eq. (11)) as

$$W(\xi_1, \xi_2, \xi_3) = p(\xi_1) \Psi_s + \bar{\kappa}_2^{(1)} (\Psi_{21} - \Psi_{21}^t) + \bar{\kappa}_3^{(1)} (\Psi_{31} - \Psi_{31}^t). \tag{89}$$

Here, $p(\xi_1)$ is the warping amplitude and an additional unknown finite strain parameter.

A1.7. The end support conditions for warping

There are two possible end conditions for warping- *wholly restrained* and the *unrestrained*. Wholly restrained warping implies $W = 0$ at the end support. Unrestrained warping would eliminate a contribution of warping to the stress component σ_{11} at the end support resulting in $W_{,\xi_1} = 0$. If a solution of form (79) is used, we can obtain the warping end conditions by imposing the following

$$\begin{aligned} \text{Warping wholly restrained: } &\bar{\kappa}_1^{(p)} = 0; \bar{\kappa}_2^{(q)} = 0 \text{ and } \bar{\kappa}_3^{(q)} = 0 \\ &\text{for all even } p \geq 0 \text{ and for all odd } q \geq 1. \\ \text{Warping unrestrained: } &\bar{\kappa}_1^{(p)} = 0; \bar{\kappa}_2^{(q)} = 0 \text{ and } \bar{\kappa}_3^{(q)} = 0 \\ &\text{for all odd } p \geq 1 \text{ and for all even } q \geq 2. \end{aligned} \tag{90}$$

A1.8. An alternative way of arriving at the end support conditions for warping

Consider an end support condition with warping unrestrained. Such a warping function must satisfy $W_{,\xi_1} = 0$ for all the material points (ξ_2, ξ_3) across the cross-section of end support. Let us call this as *unrestrained warping condition*. Differentiating Eq. (68b), with respect to the arc-length ξ_1 , we get

$$W_{,n}^{(1)} = -\bar{\kappa}_1^{(1)} t + \left\{ \nu C_2 \int_{\blacksquare} W^{(3)} d\xi_2 d\xi_3 \right\} \tilde{t}. \tag{91}$$

As an implication of *unrestrained warping condition*, we have $W_{,n}^{(1)} = 0$. This can be guaranteed from Eq. (91) if

$$\bar{\kappa}_1^{(1)} = 0 \text{ and } \int_{\blacksquare} W^{(3)} d\xi_2 d\xi_3 = 0, \tag{92}$$

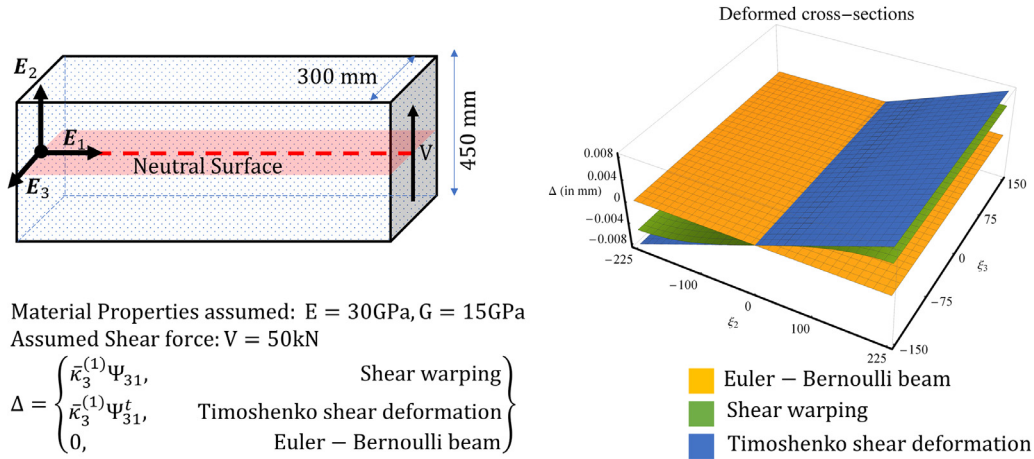
at the end support. Eq. (92) is a part of much larger set of end conditions. To proceed further, we take the derivative of Eq. (68a) with respect to ξ_1 and use the previous result (92), obtaining

$$W^{(3)} + \frac{1}{C_1} \nabla^2 W^{(1)} = \frac{1}{C_1} (\xi_2 \bar{\kappa}_3^{(2)} - \xi_3 \bar{\kappa}_2^{(2)}). \tag{93}$$

Once again, as a result of *unrestrained warping condition*, we have $\nabla^2 W^{(1)} = 0$. This result coupled with Eq. (93), implies $W^{(3)} = \frac{1}{C_1} (\xi_2 \bar{\kappa}_3^{(2)} - \xi_3 \bar{\kappa}_2^{(2)})$, which is identically satisfied if

$$W^{(3)} = 0, \bar{\kappa}_2^{(2)} = 0 \text{ and } \bar{\kappa}_3^{(2)} = 0. \tag{94}$$

We can continue the process of obtaining odd derivatives of Eqs. (68a) and (68b) with respect to ξ_1 and proceed along the same reasoning used to obtain Eqs. (92) and (94) to arrive at the end condition for the case of *unrestrained warping* as described in Eq. (90). In the very same way, we can obtain the set of end conditions for *warping wholly restrained*.



Material Properties assumed: $E = 30\text{GPa}$, $G = 15\text{GPa}$
 Assumed Shear force: $V = 50\text{kN}$

$$\Delta = \begin{cases} \bar{\kappa}_3^{(1)} \Psi_{31}, & \text{Shear warping} \\ \bar{\kappa}_3^{(1)} \Psi_{31}^t, & \text{Timoshenko shear deformation} \\ 0, & \text{Euler – Bernoulli beam} \end{cases}$$

Fig. A1. Example of shear deformation of the cross-section in the beam subjected to plane bending.

A1.9. Solution approach 2: Solution of warping function using trigonometric series

The warping function W depends on the curvatures and the end support conditions. For a small (linear) deformation, we define the component of the displacement field $v_1(\xi_1)$, $v_2(\xi_1)$, $v_3(\xi_1)$ that represents the motion of the midcurve due to axial deformation and bending. For small deformations, $v_{1,\xi_1} = e(\xi_1)$, $v_{2,\xi_1\xi_1} = \bar{\kappa}_3$ and $v_{3,\xi_1\xi_1} = -\bar{\kappa}_2$. Secondly if θ represents the angular rotation due to torsion, then $\theta_{,\xi_1} = \bar{\kappa}_1(\xi_1)$. To demonstrate the solution procedure of the modified consistent differential Eqs. (68a) and (68b) using trigonometric series, we assume simple support at the end as in Brown and Burgoyne (1994). The admissible end conditions for small deformation are

$$\begin{aligned} \theta = v_2 = v_3 = 0 \text{ at } \xi_1 = 0, L_0; \\ M_2 = M_3 = 0 \text{ at } \xi_1 = 0, L_0. \end{aligned} \tag{95}$$

Since, the consistent governing equation does not explicitly depend on the axial strain, we ignore the admissibility of the deformation field $v_1(\xi_1)$. We choose the strain parameters such that the displacement and force boundary conditions are satisfied.

$$\begin{aligned} \bar{\kappa}_1(\xi_1) &= \sum_{m=1}^{\infty} k_{1m} \cos\left(\frac{m\pi\xi_1}{L_0}\right); \\ \bar{\kappa}_2(\xi_1) &= \sum_{m=1}^{\infty} k_{2m} \sin\left(\frac{m\pi\xi_1}{L_0}\right); \\ \bar{\kappa}_3(\xi_1) &= \sum_{m=1}^{\infty} k_{3m} \sin\left(\frac{m\pi\xi_1}{L_0}\right); \end{aligned}$$

$$W(\xi_1, \xi_2, \xi_3) = \Psi_0(\xi_2, \xi_3) + \sum_{m=1}^{\infty} \Psi_m(\xi_2, \xi_3) \cos\left(\frac{m\pi\xi_1}{L_0}\right). \tag{96}$$

Substituting Eq. (96) into the equation set (68a) and (68b) and observing the orthogonality of trigonometric functions leads to the following,

Governing equation for Ψ_0 :

$$\nabla^2 \Psi_0 = 0 \text{ on } \blacksquare(\xi_1) \text{ with } \Psi_{0,n} = 0 \text{ on } \Gamma(\xi_1). \tag{97}$$

Following similar reasoning as above, $\Psi_0 = 0$, to avoid any rigid body contribution due to warping.

Governing equation for Ψ_m with $m \geq 1$:

$$\nabla^2 \Psi_m - C_1 \left(\frac{m^2 \pi^2}{L_0^2}\right) \Psi_m = C_1 \left(\frac{m\pi}{L_0}\right) (k_{3m} \xi_2 - k_{2m} \xi_3) + C_2 \bar{\lambda} \left(\frac{m^2 \pi^2}{L_0^2}\right) \int_{\blacksquare} \Psi_m d\xi_2 d\xi_3 \text{ on } \blacksquare(\xi_1); \tag{98a}$$

$$\Psi_{m,n} = -k_{1m} t - \left\{ C_2 v \left(\frac{m^2 \pi^2}{L_0^2}\right) \int_{\blacksquare} \Psi_m d\xi_2 d\xi_3 \right\} \tilde{t} \text{ on } \Gamma(\xi_1). \tag{98b}$$

The integral $\int_{\blacksquare} \Psi_m d\xi_2 d\xi_3$ can be obtained from the e_{ξ_1} field, by substituting the warping function as in Eq. (96) into the inconsistency condition (65) and utilizing the orthogonality relationship of trigonometric functions,

$$I_m(\xi_1) = \int_{\blacksquare} \Psi_m d\xi_2 d\xi_3 = \left(\frac{\tilde{\lambda} - 2v\lambda}{\tilde{\lambda}}\right) \left(\frac{L_0^2}{m^2 \pi^2}\right) A(\xi_1) \sec\left(\frac{m\pi\xi_1}{L_0}\right) \int_0^{L_0} e_{\xi_1} \left(\cos\frac{m\pi\xi_1}{L_0}\right) d\xi_1. \tag{99}$$

Similarly, the Fourier coefficients k_{1m} , k_{2m} and k_{3m} can be obtained as,

$$k_{1m} = \frac{2}{L_0} \int_0^{L_0} \bar{\kappa}_1(\xi_1) \cos\left(\frac{m\pi\xi_1}{L_0}\right) d\xi_1; \tag{100a}$$

$$k_{2m} = \frac{2}{L_0} \int_0^{L_0} \bar{\kappa}_2(\xi_1) \sin\left(\frac{m\pi\xi_1}{L_0}\right) d\xi_1; \tag{100b}$$

$$k_{3m} = \frac{2}{L_0} \int_0^{L_0} \bar{\kappa}_3(\xi_1) \sin\left(\frac{m\pi\xi_1}{L_0}\right) d\xi_1. \tag{100c}$$

Check for consistency of Eqs. (98a) and (98b):

Using Eq. (98b), Gauss theorem and the results in Eqs. (60a) and (60b), we have,

$$\begin{aligned} \int_{\blacksquare} \nabla^2 \Psi_m d\xi_2 d\xi_3 &= \oint \Psi_{m,n} d\Gamma \\ &= -k_{1t} \oint t d\Gamma - \left\{ C_2 v \left(\frac{m^2 \pi^2}{L_0^2}\right) \int_{\blacksquare} \Psi_m d\xi_2 d\xi_3 \right\} \oint \tilde{t} d\Gamma \\ &= -\left\{ 2vAC_2 \left(\frac{m^2 \pi^2}{L_0^2}\right) \int_{\blacksquare} \Psi_m d\xi_2 d\xi_3 \right\}. \end{aligned} \tag{101}$$

Integrating Eq. (98a) across the cross-section $\blacksquare(\xi_1)$, we have,

$$\int_{\blacksquare} \nabla^2 \Psi_m d\xi_2 d\xi_3 = C_1 \left(\frac{m^2 \pi^2}{L_0^2} \right) \int_{\blacksquare} \Psi_m d\xi_2 d\xi_3 + C_1 \left(\frac{m\pi}{L_0} \right) \left(k_{3m} \int_{\blacksquare} \xi_2 d\xi_2 d\xi_3 - k_{2m} \int_{\blacksquare} \xi_3 d\xi_2 d\xi_3 \right) + C_2 A \bar{\lambda} \left(\frac{m^2 \pi^2}{L_0^2} \right) \int_{\blacksquare} \Psi_m d\xi_2 d\xi_3 = (C_2 A \bar{\lambda} + C_1) \left(\frac{m^2 \pi^2}{L_0^2} \right) \int_{\blacksquare} \Psi_m d\xi_2 d\xi_3. \tag{102}$$

The consistency between Eqs. (98a) and (98b) can be proved from Eqs. (101) and (102), if we can show that $C_1 + C_2 A \bar{\lambda} = -2\nu A C_2$. Using the definitions of C_1 , C_2 , and $\bar{\lambda}$, we have

$$C_1 + C_2 A \bar{\lambda} = \frac{\tilde{\lambda}}{G} - \left(\frac{\tilde{\lambda} + 2\nu(G - \tilde{\lambda})}{G} \right) \left(\frac{\tilde{\lambda}}{\tilde{\lambda} - 2\nu\lambda} \right) = 2 \left(\frac{\nu \tilde{\lambda}}{\tilde{\lambda} - 2\nu\lambda} \right) = -2\nu A C_2. \tag{103}$$

Therefore, the governing differential equations for Ψ_m are consistent.

Solving for Ψ_m :

Consider a solution of the form

$$\Psi_m = \Psi_{0m} + \sum_{i=1}^3 \Psi_{im} k_{im}. \tag{104}$$

The functions Ψ_{jm} for $j = 0 - 3$ satisfies four set of differential equations. The governing differential equations for Ψ_{0m} are,

$$\nabla^2 \Psi_{0m} - C_1 \left(\frac{m^2 \pi^2}{L_0^2} \right) \frac{\tilde{\lambda}}{G} \Psi_{0m} = C_2 \bar{\lambda} \frac{m^2 \pi^2}{L_0^2} I_m(\xi_1) \text{ at } \blacksquare(\xi_1); \tag{105a}$$

$$\Psi_{0m,n} = -C_2 \nu \left(\frac{m^2 \pi^2}{L_0^2} \right) I_m(\xi_1) \tilde{t} \text{ at } \Gamma(\xi_1). \tag{105b}$$

The governing differential equations for Ψ_{1m} are,

$$\nabla^2 \Psi_{1m} - C_1 \left(\frac{m^2 \pi^2}{L_0^2} \right) \frac{\tilde{\lambda}}{G} \Psi_{1m} = 0 \text{ at } \blacksquare(\xi_1); \tag{106a}$$

$$\Psi_{1m,n} = -t \text{ at } \Gamma(\xi_1). \tag{106b}$$

The governing differential equations for Ψ_{2m} are,

$$\nabla^2 \Psi_{2m} - C_1 \left(\frac{m^2 \pi^2}{L_0^2} \right) \frac{\tilde{\lambda}}{G} \Psi_{2m} = -C_1 \left(\frac{m\pi}{L_0} \right) \xi_3 \text{ at } \blacksquare(\xi_1); \tag{107a}$$

$$\Psi_{2m,n} = 0 \text{ at } \Gamma(\xi_1). \tag{107b}$$

The governing differential equations for Ψ_{3m} are,

$$\nabla^2 \Psi_{3m} - C_1 \left(\frac{m^2 \pi^2}{L_0^2} \right) \frac{\tilde{\lambda}}{G} \Psi_{3m} = C_1 \left(\frac{m\pi}{L_0} \right) \xi_2 \text{ at } \blacksquare(\xi_1); \tag{108a}$$

$$\Psi_{3m,n} = 0 \text{ at } \Gamma(\xi_1). \tag{108b}$$

We can obtain the functions Ψ_{jm} with $j = 0 - 4$ by solving the equation set (105a)-(108b). Therefore, the warping function W can be obtained using Eq. (96), the Fourier coefficients as defined in equation set (100a)-(100c) and (104).

In this appendix, we have detailed the first stage of geometric coupling between axial deformation, Poisson's effect and warping. Our novel aim to obtain a *simplified but refined* warping model to

develop comprehensive kinematics (such that we retain the single manifold nature of the kinematics) leads to an *inconsistent warping equation*. Elimination of inconsistency result in *consistent differential equations for warping* that can be solved. For $\nu = 0$, the presented theory of warping reduces to the theory presented by Burgoyne and Brown (1994) and Brown and Burgoyne (1994).

A2. The vector λ_i^j for various deformed configurations

For the deformed state Ω_1

$$\lambda_1^1 = (((1 + e) \cos \gamma_{11} - 1) + \xi_3 \bar{\kappa}_2 - \xi_2 \bar{\kappa}_3) \mathbf{d}_1 + ((1 + e) \sin \gamma_{12} - \xi_3 \bar{\kappa}_1) \mathbf{d}_2 + ((1 + e) \sin \gamma_{13} + \xi_2 \bar{\kappa}_1) \mathbf{d}_3; \lambda_2^1 = \lambda_3^1 = \mathbf{0}.$$

For the deformed state Ω_2

$$\lambda_1^2 = (((1 + e) \cos \gamma_{11} - 1) + \xi_3 \bar{\kappa}_2 - \xi_2 \bar{\kappa}_3 + W_{,\xi_1}) \mathbf{d}_1 + ((1 + e) \sin \gamma_{12} - \xi_3 \bar{\kappa}_1 + W \bar{\kappa}_3) \mathbf{d}_2 + ((1 + e) \sin \gamma_{13} + \xi_2 \bar{\kappa}_1 - W \bar{\kappa}_2) \mathbf{d}_3; \lambda_2^2 = W_{,\xi_2} \mathbf{d}_1; \lambda_3^2 = W_{,\xi_3} \mathbf{d}_1.$$

A3. The vector λ_1^{rj} for various deformed configurations

$$\lambda_1^{r1} = \left(\frac{1}{\xi_3 \bar{\kappa}_{0_2} - \xi_2 \bar{\kappa}_{0_3}} \right) (((1 + e) \cos \gamma_{11} - 1) + \xi_3 (\bar{\kappa}_2 - \bar{\kappa}_{0_2}) - \xi_2 (\bar{\kappa}_3 - \bar{\kappa}_{0_3})) \mathbf{d}_1 + ((1 + e) \sin \gamma_{12} - \xi_3 \bar{\kappa}_1) \mathbf{d}_2 + ((1 + e) \sin \gamma_{13} + \xi_2 \bar{\kappa}_1) \mathbf{d}_3.$$

$$\lambda_1^{r2} = \left(\frac{1}{\xi_3 \bar{\kappa}_{0_2} - \xi_2 \bar{\kappa}_{0_3}} \right) (((1 + e) \cos \gamma_{11} - 1) + \xi_3 (\bar{\kappa}_2 - \bar{\kappa}_{0_2}) - \xi_2 (\bar{\kappa}_3 - \bar{\kappa}_{0_3}) + W_{,\xi_1}) \mathbf{d}_1 + ((1 + e) \sin \gamma_{12} - \xi_3 \bar{\kappa}_1 + W \bar{\kappa}_3) \mathbf{d}_2 + ((1 + e) \sin \gamma_{13} + \xi_2 \bar{\kappa}_1 - W \bar{\kappa}_2) \mathbf{d}_3.$$

$$\lambda_1^{r3} = \left(\frac{1}{\xi_3 \bar{\kappa}_{0_2} - \xi_2 \bar{\kappa}_{0_3}} \right) (((1 + e) \cos \gamma_{11} - 1) + \xi_3 \bar{\kappa}_2 - \xi_3 \bar{\kappa}_{0_2} - \xi_2 \bar{\kappa}_3 + \xi_2 \bar{\kappa}_{0_3} + W_{,\xi_1}) \mathbf{d}_1 + ((1 + e) \sin \gamma_{12} - \xi_3 \bar{\kappa}_1 + W \bar{\kappa}_3) \mathbf{d}_2 + ((1 + e) \sin \gamma_{13} + \xi_2 \bar{\kappa}_1 - W \bar{\kappa}_2) \mathbf{d}_3.$$

A4. Deformation gradient tensor referenced to another deformed state

We consider a deformation of class Ω_3 . Suppose \mathbf{F}_{3_p} and \mathbf{F}_{3_q} represent the deformation gradient tensor of a deformed state Ω_{3_p} and Ω_{3_q} respectively, referenced to the undeformed state Ω_{0_0} . If $\{\mathbf{d}_{p_i}\}$ and $\{\mathbf{d}_{q_i}\}$ represent the director triad for the configurations Ω_{3_p} and Ω_{3_q} , we have, $\mathbf{Q}_p = \mathbf{d}_{p_i} \otimes \mathbf{E}_i$ and $\mathbf{Q}_q = \mathbf{d}_{q_i} \otimes \mathbf{E}_i$ (sum on i). We obtain the deformation gradient tensor $\mathbf{F}_{3_{qp}}$ of the state Ω_{3_q} referenced to Ω_{3_p} as

$$\mathbf{F}_{3_{qp}} = \mathbf{F}_{3_q} \mathbf{F}_{3_p}^{-1}$$

where,

$$\mathbf{F}_{3_p} = \lambda_i^{3p} \otimes \mathbf{E}_i + \mathbf{Q}_p; \mathbf{F}_{3_q} = \lambda_i^{3q} \otimes \mathbf{E}_i + \mathbf{Q}_q.$$

In the equation above, λ_i^{3p} and λ_i^{3q} represent the strain vectors related to the configuration Ω_{3p} and Ω_{3q} respectively.

It is interesting to note that unlike the deformation gradient matrix $[\nabla_{\Omega_{00}} \mathbf{u}_0]_{\mathbf{d}_{p_l} \otimes \mathbf{E}_m}$, the matrix $[\nabla_{\Omega_{00}} \mathbf{u}_p]_{\mathbf{d}_{p_l} \otimes \mathbf{E}_m} = [\lambda_1^{3p} \otimes \mathbf{E}_1]_{\mathbf{d}_{p_l} \otimes \mathbf{E}_m} + [\lambda_2^{3p} \otimes \mathbf{E}_2]_{\mathbf{d}_{p_l} \otimes \mathbf{E}_m} + [\lambda_3^{3p} \otimes \mathbf{E}_3]_{\mathbf{d}_{p_l} \otimes \mathbf{E}_m}$ has maximum rank 3. It has rank 3 and is nonsingular if $\langle \lambda_1^{3p}, \mathbf{d}_{p_1} \rangle \neq 0$, $\langle \lambda_2^{3p}, \mathbf{d}_{p_2} \rangle \neq 0$ and $\langle \lambda_3^{3p}, \mathbf{d}_{p_3} \rangle \neq 0$. Here the index l and m are used to represent the frames. Therefore, the expression for \mathbf{F}_{3p}^{-1} can not be obtained from Eq. 1 in Miller (1981). Consider the case where the matrix $[\nabla_{\Omega_{00}} \mathbf{u}_p]_{\mathbf{d}_{p_l} \otimes \mathbf{E}_m}$ has rank 3 and is nonsingular. The fact that the matrix $[\lambda_1^{3p} \otimes \mathbf{E}_1]_{\mathbf{d}_{p_l} \otimes \mathbf{E}_m}$, $[\lambda_2^{3p} \otimes \mathbf{E}_2]_{\mathbf{d}_{p_l} \otimes \mathbf{E}_m}$ and $[\lambda_3^{3p} \otimes \mathbf{E}_3]_{\mathbf{d}_{p_l} \otimes \mathbf{E}_m}$ are rank 1 and non-singular allows us to use the theorem in page 69 of Miller (1981) to arrive at the expression for \mathbf{F}_{3p}^{-1} .

References

- Altenbach, H., Biršan, M., Eremeyev, M., 2012. On a thermodynamic theory of rods with two temperature fields. *Acta Mech.* 223, 1583–1596.
- Altenbach, H., Eremeyev, V.A., 2013. *Generalized Continua from Theory to Engineering Applications*. CISM Courses and Lectures, Vol. 541. Springer, New York.
- Antman, S.S., 1972. *The Theory of Rods*. Handbuch der Physik, Vol. VIa/2. Springer, Berlin.
- Antman, S.S., 1974. Kirchhoff's problem for nonlinearly elastic rod. *Q. Appl. Math.* 32, 221–240.
- Antman, S.S., 1995. *Nonlinear Problems of Elasticity*. Springer, New York.
- Asaro, R., Lubarda, V.A., 2006. *Mechanics of solids and materials*. Cambridge University Press, NY. First edition.
- Biršan, M., Altenbach, H., 2011. On the theory of porous elastic rods. *Int. J. Solids Struct.* 48, 910–924.
- Brand, M., Rubin, M.B., 2007. A constrained theory of a Cosserat point for numerical solution of dynamic problems of non-linear elastic rods with rigid cross-sections. In: *Proceedings of Royal Society, Vol. 337A*, pp. 485–507. London.
- Brown, E.H., Burgoyne, C.J., 1994. Nonuniform elastic torsion and flexure of members with asymmetric cross-section. *Int. J. Mech. Sci.* 36, 39–48.
- Burgoyne, C.J., Brown, E.H., 1994. Nonuniform elastic torsion. *Int. J. Mech. Sci.* 36, 23–38.
- Chadha, M., Todd, M.D., 2017a. A generalized approach to reconstructing the three-dimensional shape of slender structures including the effects of curvature, shear, torsion, and elongation. *ASME J. Appl. Mech.* 84, 041003–1–041003–11.
- Chadha, M., Todd, M.D., 2017b. An introductory treatise on reduced balance laws of Cosserat beams. *Int. J. Solids Struct.* 126–127, 54–73.
- Chadha, M., Todd, M.D., 2018a. A Displacement Reconstruction Strategy for Long, Slender Structures from Limited Strain Measurements and Its Application to Underground Pipeline Monitoring. In: Conte, J., Astroza, R., Benzoni, G., Feltrin, G., Loh, K., Moaveni, B. (Eds.), *Experimental Vibration Analysis for Civil Structures*. EVACES 2017. Lecture Notes in Civil Engineering, 5. Springer, Cham, pp. 317–327.
- Chadha, M., Todd, M.D., 2018b. An Improved Shape Reconstruction Methodology for Long Rod like Structure Using Cosserat Kinematics—including the Poisson's Effect. *Nonlinear Dynamics, Volume 1*, conference proceedings of the Society for Experimental Mechanics Series, Kerschen G., Chapter 25.
- Cohen, H., 1966. A non-linear theory of elastically directed curve. *Int. J. Eng. Sci.* 4, 511–524.
- Cosserat, E., Cosserat, F., 1909. *Theorie des Corps Deformable*. Herman, Paris.
- Do Carmo, M.P., 1992. *Riemannian geometry*. Birkhäuser, Second edition Boston, USA.
- Duhem, P., 1893. Le potentiel thermodynamique et la pression hydrostatique. *Annales ecole norm.* 10, 183–230.
- Elter, E., 1983. Two formulii of the shear center. *Periodica Polytechnica Mechanical Engineering* 28, 179–193.
- Ericksen, J.L., Truesdell, C., 1958. Exact theory of stress and strain in rods and shells. *Arch. Rational Mech. Analysis* 1, 295–323.
- Fang, Y., 2005. A geometrically exact thin-walled beam theory considering in-plane cross-section distortion. Cornell University Ph.D. dissertation.
- Friedman, A., Todd, M.D., Kirkendall, K., Tveten, A., Dandridge, A., 2003. Rayleigh backscatter-based fiber optic distributed strain sensor with tunable gage length. In: *SPIE Smart Structures/NDE 5050 Proceedings*, pp. 2–6.
- Gjelsvik, A., 1981. *The theory of thin walled bars*. Wiley, New York.
- Goodier, J.N., 1941. The buckling of compressed bars by torsion and flexure. *Cornell University Engineering Experimental Station* 84, 27.
- Green, A.E., Naghdi, P.M., Wener, M.L., 1974. On Theory of Rods I: Derivations from the Three-dimensional Equations. In: *Proceedings of Royal Society, Vol. 337A*, pp. 451–483. London.
- Green, A.E., Naghdi, P.M., Wener, M.L., 1974. On theory of rods II: Derivations by direct approach. In: *Proceedings of Royal Society, Vol. 337A*, pp. 485–507. London.
- Hay, G.E., 1942. The finite displacement of thin rods. *Trans. Am. Math. Soc.* 51, 65–102.
- Iura, M., Atluri, S.N., 1989. On a consistent theory, and variational formulation of finitely stretched and rotated 3-d space-curved beam. *Comput. Mech.* 4, 73–88.
- Kapania, R.K., Li, J., 2003. On geometrically exact curved beam theory under rigid cross-section assumption. *Comput. Mech.* 30, 428–443.
- Lin, W.Y., Hsiao, K.M., 2003. More general expression for the torsional warping of a thin-walled open-section beam. *Int. J. Mech. Sci.* 45, 831–849.
- Maugin, G.A., 2017. *Non-Classical Continuum Mechanics - A Dictionary*. Springer, Singapore.
- Meier, C., Popp, A., Wall, W.A., 2017. Geometrically exact finite element formulations for slender beams: kirchhoff-love theory versus simo-reissner theory. *Arch. Comput. Methods Eng.* doi:10.1007/s11831-017-9232-5.
- Miller, K.S., 1981. On the inverse of the sum of matrices. *Mathematics Magazine* 54, 67–72.
- Naghdi, P.M., Rubin, M.B., 1982. Constrained theory of rods. *J. Elast.* 14, 343–361.
- Reissner, E., 1972. On one-dimensional finite-strain beam theory: the plane problem. *J. Appl. Math. Phys.* 23, 795–804.
- Reissner, E., 1973. On one-dimensional large displacement finite beam theory. *Studies in Applied Mechanics* 52, 87–95.
- Reissner, E., 1981. On finite deformation of space curved beams. *J. Appl. Math. Phys.* 32, 734–744.
- Rubin, M.B., 2000. *Cosserat Theories: Shells, Rods and Points*. Kluwer Academic Publishers, The Netherlands.
- Schutz, B., 2009. *A First Course in General Relativity*. Cambridge University Press, UK.
- Simo, J.C., 1985. A finite beam formulation. the three dimensional dynamic problem. part 1. *Comput. Methods Appl. Mech. Eng.* 49, 55–70.
- Simo, J.C., Vu-Quoc, L., 1991. A geometrically exact rod model incorporating shear and torsion- warping deformation. *Int. J. Solids Struct.* 27, 371–393.
- Sokolnikoff, I.S., 1956. *Mathematical theory of elasticity*. McGraw-Hill, New York.
- Svetlitsky, V.A., 2000. *Statics of Rods*. Springer, New York.
- Svetlitsky, V.A., 2004. *Dynamics of Rods*. Springer, New York.
- Timoshenko, S.P., 1921. On the correction for shear of the differential equation for transverse vibrations of prismatic beams. *Philoso. Mag. J. Sci.* 41, 744–746.
- Todd, M.D., Skull, C.J., Dickerson, M., 2013. A local material basis solution approach to reconstructing the three-dimensional displacement of rod-like structure from strain measurements. *ASME J. Appl. Mech.* 80, 041028–1–041003–10.
- Trefftz, E.Z., 1935. Die bestimmung der knicklast gedruckter, rechteckiger platten. *ZAMM* 15, 339–344.
- Vlasov, V.Z., 1961. *Thin walled elastic beams*, english translation published for US science foundation by Israel program for scientific translation.
- Whitman, A.B., DeSilva, C.N., 1969. A dynamical theory of elastic directed curves. *ZAMP* 20, 200–212.